Strategies to Enhance Drug Loading and Functionality in Polymeric Ultrasound Contrast Agents

A Thesis

Submitted to the Faculty

of

Drexel University

by

Mi Thant Mon Soe

in partial fulfillment of the

requirements for the degree

of

Master of Science in Biomedical Engineering

September 2014

Acknowledgements

Firstly, I would like to acknowledge Dr. Wheatley for her guidance, patience and input throughout the process. She has given me an unforgettable research experience and a basement full of awesome lab mates. I have known her from my first freshmen class, when she waltzed into the freshmen engineering lab with unbound enthusiasm. For the past five years, she has continually cheered me up with her gigantic, bubbly personality; making her an integral part of my Drexel experience.

I would also like to thank my committee members: Dr. John Eisenbrey and Dr. Sriram Balasubramanian for their time, wisdom and interest in my research. In addition, I need to thank in particular Tarn Teraphongphom, Lauren Jablonowski, Reva Street and Dr. Michael Cochran for teaching and inspiring my work in the basement. I would also like to thank the previous students from the Wheatley lab who have worked on the standard fabrication, and testing protocols that I had an opportunity to utilize for my project. Furthermore, I would like to thank the other undergraduate students from my lab - Nick Daroshefski, David Brown and Lorenzo Albala, and friends from other labs who have made my thesis work possible through their assistance.

Finally, I would like to thank my most caring, wonderful and amazing parents, the rest of the family, all of my friends and the e-board of the International Students Union for their love and support. I am grateful that they have never given up on me; especially, my best friends, Giang Nguyen and Ian Kennedy. Collectively, I would like to thank every single person who has touched and shaped the current Thant, who was able to complete this master thesis.

Table of contents

List of Figures

List of Tables

List of Abbreviations

Aq: Aqueous

DI water: Deionized water

DMSO: Dimethyl sulfoxide

Dox: Doxorubicin

EPR: Enhanced permeation and retention

h-Dox: hydrophobic Doxorubicin

IPA: Isopropyl alcohol

MNP: Magnetic nanoparticles

MNP-OA: Magnetic nanoparticles capped with oleic acid

MNP-OA-PA: Magnetic nanoparticles capped with oleic acid coated in Pluronic acid

MRI: Magnetic resonance imaging

MeCl: Methylene chloride

MW: Molecular weight

PBS: Phosphate buffered saline

PDI: Poly dispersity index

PLA: Poly (lactic acid)

PVA: Poly (vinyl alcohol)

SEM: Scanning electron microscopy

TEA: Triethylamine

UCA: Ultrasound contrast agents

VSM: Vibrating sample magnetometer

Abstract

Strategies to Enhance Drug Loading and Functionality in
Polymeric Ultrasound Contrast Agents
Mi Thant Mon Soe
Margaret A. Wheatley, Ph.D.

Ultrasound contrast agents (UCA) are currently studied to further improve their diagnostic capabilities and for better targeted delivery of genes and drugs, with a strong focus on cancer therapy. These injectable microbubbles that strongly interact with ultrasound can be loaded with chemotherapeutic drugs, such as hydrophilic Doxorubicin-HCl (Dox-HCl), for successful targeted delivery upon rupturing under focused ultrasound. This reduces the harmful side effects of chemotherapeutic drugs that are administered systemically. Previous studies with UCA made from poly (lactic acid) (PLA) have shown maximum drug loading of 6.2 mg Dox-HCl/ g PLA at an initial loading concentration of 30 mg Dox-HCl/ g PLA. In order to increase the treatment efficiency, Dox loaded magnetic iron oxide nanoparticles (MNP) were encapsulated within the PLA shell. The inclusion of the MNP not only allows for increased Dox loading, but also provides more imaging capabilities, since MNP can be imaged using magnetic resonance imaging (MRI) even after ultrasound-induced rupture of UCA.

Preliminary *in vitro* tests were performed to determine methods of maintaining the highest amount of ultrasound interaction, measured by acoustic enhancement, possible for magnetic nanoparticles capped with oleic acid (MNP-OA) loaded UCA. This was seen at 33wt% MNP-OA loading where the enhancement reached 14.77±0.61 dB.

The magnetic nanoparticles had a short shelf life and so, the MNP-OA were further coated with Pluronic acid to form MNP-OA-PA. The hydrophobic Dox (h-Dox), formed after removing the HCl, was loaded onto the MNP, between the oleic acid chains. However, there was a low entrapment of 2.88 μg Dox/ mg MNP. When these MNP-OA-PA were loaded onto the UCA, the resulting UCA were non-echogenic. The problem was identified by loading just the Pluronic acid onto the UCA, which showed that UCA lose their echogenicity when formed in the presence of Pluronic acid. Low loading of Dox onto the MNP-OA together with the decreased acoustic enhancements made the design of Dox-loaded MNP-OA-PA encapsulated in UCA less than was hoped for.

After the Dox-HCl was modified to make it more hydrophobic, they were loaded onto PLA UCA to determine whether the drug payload would increase since PLA is also hydrophobic. It was found that in the hydrophobic form, a maximum drug load of 27.18±0.39 mg Dox / g PLA can be achieved upon initial loading of 30 mg Dox / g PLA for the 3wt% h-Dox loading, resulting in a significant increase ($p<0.0001$) in drug payload when compared to Dox-HCl loading. The highest acoustic enhancement of 12.69±0.81dB was seen at the largest dose recorded (15.3 μg/mL) for the *in vitro* acoustic enhancement experiment. This increase in drug encapsulation would allow a higher dose of doxorubicin to be delivered to the patient while maintaining the desired acoustic characteristics.

1. INTRODUCTION

Cancer is a leading cause of death worldwide and according to the International Agency for Research on Cancer, in 2012 alone, there were 8.2 million deaths [1]. This includes deaths from liver cancer (745 000 deaths) and breast cancer (521 000 deaths) [1]. Early detection of breast cancer, followed by chemotherapy can reduce recurrence and increase survival rates by at least 45% [2]. Liver cancer is the sixth leading cause of death in the world and its occurrence is higher in Southeast Asia and Africa where there is a higher number of patients with hepatitis B and C, both of which can lead to liver cancer. [3]. These two diseases that are closely associated with liver cancer are mainly treated by resection. In such underdeveloped areas of the world, only a small portion of the population can afford to get a surgical intervention. Chemotherapy is another form of treatment that is available and is cheaper.

One of the main problems with chemotherapy is that it requires a cocktail of medications that work synergistically to kill the tumor cells over a period of time [4]. Unfortunately, these drugs can also kill the healthy cells, causing multiple side effects that make the patient weaker. In order to reduce these side effects, several targeted drug delivery designs have been formulated [5-7]. One of these designs previously developed in the Wheatley lab utilizes polymeric UCA which can be shattered using ultrasound [8]. These contrast agents were loaded with chemotherapeutic drugs such as doxorubicin (Dox) into their PLA shells and injected intravenously into the patient. Focused ultrasound waves can be used to shatter these drug loaded UCA near the tumor site, allowing more drug to reach the tumor cells, while avoiding healthy cells.

This project aims to increase the drug payload of the chemotherapeutic agent – Dox on the PLA UCA so that it may be possible to deliver a higher dose of the Dox to the tumor while administering the same amount of UCA, reducing systemic effects. In order to do this, Dox would be loaded onto magnetic nanoparticles (MNP) to increase the surface area onto which it can attach to. These Dox-MNP can then be encapsulated onto the PLA shell, increasing the overall Dox loading onto the UCA without compromising the acoustic properties (Figure 1-1).

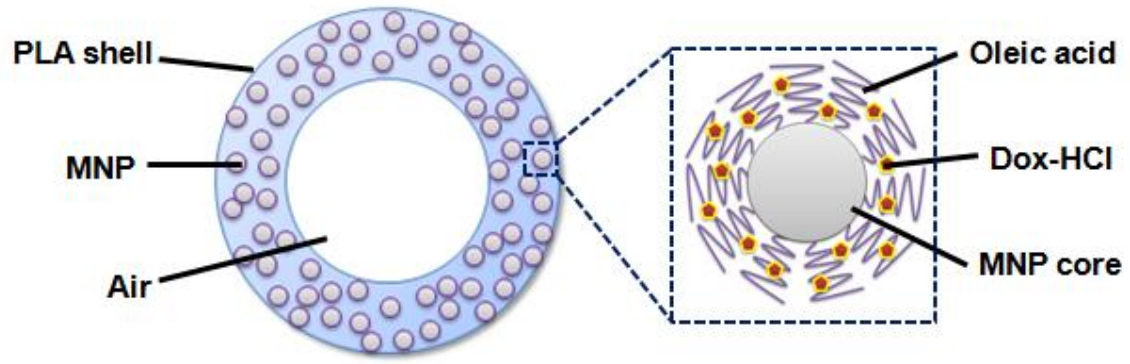

Figure 1-1 Proposed structure of the poly (lactic acid) ultrasound contrast agent loaded with magnetic nanoparticles

Overall Design Objective

To increase the loading of the chemotherapeutic Doxorubicin onto the poly (lactic acid) shell UCA without compromising the acoustic properties of the UCA. This would decrease the systemic side effects of Dox and increase safety due to less ultrasound contrast agents being needed to achieve the same therapeutic effect.

2. BACKGROUND

2.1. Cancer and Cancer Therapies

Cancer is a general term used to refer to any condition caused by uncontrolled cell division. In 2013, it was expected that over 1 660 290 people in US would be diagnosed with cancer while 580 350 will die because of it. Between 2002 and 2008, the five years survival rate was 68% [9]. Current treatments include surgery, chemotherapy, radiation therapy, targeted therapy, immunotherapy, hyperthermia, stem cell transplant, and photodynamic therapy [10].

Treatments such as chemotherapy are used to minimize the spread of the growth and spreading of the cancer cells to other parts of the body. The drugs that are used have a systemic effect on the body and damage not just the cancer cells but also the normal ones. This results in side effects such as immunosuppression and neutropenia [11]. Another problem with chemotherapy is its low efficacy due to its inability to reach some tumor sites resulting from irregular vasculature and multidirectional blood flow around the mass and the high inter tumoral pressure [12]. Thus, targeted drug delivery was developed to ensure that the chemotherapeutic drug works only at the tumor site.

In this research, a commonly used chemotherapeutic drug, Doxorubicin (Dox) was used. Dox is an anthracycline antibiotic and has a molecular weight of 543.52 [13]. The chemical structure of Doxorubicin [16]is shown in Figure 2-1. Doxorubicin hydrochloride (Dox-HCl) is a hydrophilic form of the drug and has a molecular weight of 579.98. Dox disrupts the tumor cell proliferation by two different mechanisms. It can inhibit DNA replication by intercalating between the DNA base pairs. It also inhibits the topoisomerase II, preventing them from ligating back after the separation of the double

strands during DNA replication [14]. It has been used to treat many different cancers such as leukemia, breast, lung and thyroid carcinomas and bone sarcomas. Due to its mechanism of action, Dox also forms oxygen free radicals that lead to several reported cardiac problems such as atrial and centricular dysarrhythmias, pericardis-myocarditic syndrome, and chronic myopathy [15].

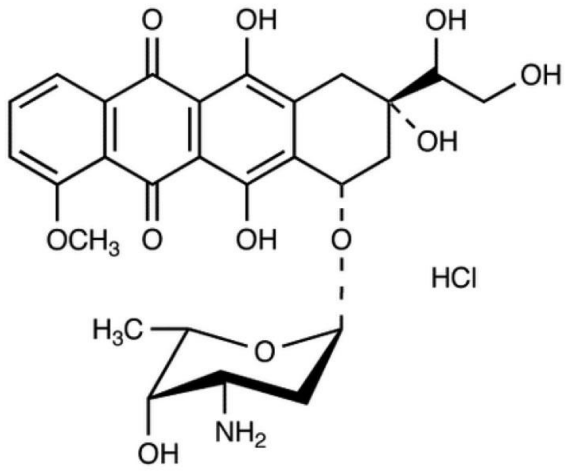

Figure 2-1 The chemical structure of Doxorubicin [16]

Others have attempted to reformulate Dox in order to reduce side effects and protect the heart. Doxil® is the FDA approved intravenous form of the drug formed by encapsulating the Dox-HCl in liposomes [17]. Due to its encapsulation within the liposome, Doxil® has a significantly decreased cardiotoxicity when compared to the unencapsulated Dox [18]. However, it has been shown to cause Palmer Plantar Erythrodysthesia (PPE), a dermal condition, and complement activation-related pseudo-allergy (CARPA), a reaction to the infusion of the Doxil® into the body. To reduce the accumulation of Doxil® to the skin which leads to PPE, the half-life of Doxil® can be reduced. In addition, a more controlled release can be done to prevent these typical side effects from occurring [19].

2.2. Ultrasound

Ultrasound imaging is widely used in medical diagnosis for its noninvasiveness and low cost. Ultrasound imaging technique is based on sound waves which are reflected or scattered by heterogeneous tissues of the human body [20]. The receiver in the transducer would detect these scattered echoes, and with image processing techniques, real-time images could be produced of fetus, cardiovascular system or tumors. The unreflected waves would be converted to thermal energy when absorbed or continue to travel through the tissue until reflected by another boundary. The heterogeneity of the tissues results in impedance mismatch, a phenomenon, caused by a difference in the density within parts of the tissue that result in a difference in the speed of the sound traveling through it. Acoustic impedance (z) is defined as:

$$z = \rho \times c \qquad \text{Eq. 1}$$

where ρ is the density (kg/m^3) of the medium and c is the speed of sound (m/s) through the medium [21].

This difference must be at a macroscopic structural scale like that of the cells in the body and not at the molecular scale. This limitation is due to the type of transducers used in medical imaging; they are around 2 to 10 Hz, generating ultrasounds of wavelengths between 150 and 800 μm [22]. This makes it extremely difficult to image blood since the blood cells and other components are smaller than these wavelengths because they have to be small enough to pass through capillaries of 7 μm in diameter. In addition, there is the Doppler effect which is caused by the frequency shift in the echoes when they are reflected by the moving blood, resulting in generation of weak signals.

2.3. Ultrasound Contrast Agents

Ultrasound contrast agents are used to enhance the ultrasound signal by effectively increasing the scattering of the sound waves from the blood, thereby increasing their probability to reach the transducer where signal reading takes place. To be small enough to pass through the small capillaries and still scatter enough ultrasound even when they are much smaller than the ultrasound wavelengths, UCA needs to be compressible. Thus, UCA are made with shells that stabilize the microbubbles, preventing the gas from dissolving into the surrounding liquid. The gas increases the impedance mismatch between the blood and the gas core mainly from the fact that the density of gas is much lower than that of water, which makes up 60% of the blood [23]. This affects the impedance which then affects the reflective coefficient (*R*) that determines the percentage of acoustic wave reflected. This relationship is defined as:

$$R = \frac{z_2 - z_1}{z_2 + z_1} \quad [21] \qquad \text{Eq. 2}$$

where z_1 is the acoustic impedance of the first medium and z_2 is the acoustic impedance of the second medium. At 1 atm and 20˚C, the z_{air} is 415 Pa·s/m while z_{water} is 1.48×10^6 Pa·s/m. Using the Eq. 2, the *R* would be approximately equal to 1, making UCA a good reflector of acoustic wave. In addition, the greater the compressibility of the UCA when compared to the surrounding tissues, the greater its ability to reflect the ultrasound wave that has a wavelength greater than its own diameter. Many different types of UCA have been designed; shells made from phospholipids, polymer or surfactants while the gas cores have ranged from air, to perfluorocarbons [24-26]. Table 1 lists the current commercially available UCA [27 -32].

Table 1. Commercially Available Ultrasound Contrast Agents [27-32]

Agent	Diameter (μm)	Core Material	Shell Material
Imagent	6	Perflexane	Phospholipid
Optison	4.7	Perfluoropropane	Albumin
Sonovue *	2.5	Sulfur hexafluoride	Phospholipid
Definity *	2.5	Octafluoropropane	Phospholipid
Sonazoid *	2.5	Perfluorobutane	Hydrogenated egg phosphatidyl serine
SonoRx †	-	Air	Simethicone coated Cellulose

* not FDA approved for use in the US but used outside the US

† discontinued

Previous studies conducted in the Wheatley lab have successfully fabricated polymer shells made of poly (lactic acid) that are filled with air which have *in vitro* acoustic enhancements of over 20 dB [8]. The mean diameter of the microbubbles is 2 μm while the thickness of the shell is between 100 to 200 nm. Poly (lactic acid), shown in Figure 2-2, is an FDA approved molecule that can be broken down into the lactic acid which is a naturally occurring biodegradable metabolite, making it a suitable molecule to be used as a UCA shell.

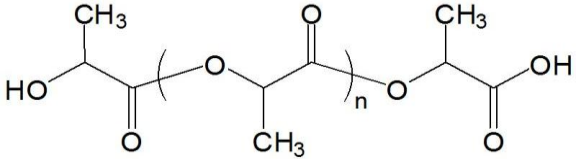

Figure 2-2 Chemical structure of poly (lactic acid) [33]

2.4. Ultrasound Assisted Chemotherapeutic Delivery

One way to achieve controlled release is through the use of ultrasound contrast agents such as encapsulated air microbubbles which are small enough (1 to 6 μm) to pass through the lumens in the small capillaries of circulatory system [34]. During insonation at the tumor site, the microbubbles oscillate about a resonant diameter and then rupture into nanoparticles that can permeate through the leaky pores of the tumor vasculature. For targeted drug delivery, the drug can be loaded into the shell whereby the nano shards created during rupture would release the drug at the site of the tumor. Also, a sustained release is ensured as the drug would be gradually released as the polymer hydrolyses. This reduces systemic side effects of the drug agent. In this research, the shell used was made from poly lactic acid (PLA). Three methods of loading the drug onto the PLA shell have been developed in the Wheatley lab [35]. The Dox can be either incorporated into the shell during the primary emulsion phase, or during the hexane washing step of the fabrication and lastly, Dox can be adsorbed onto the shell post fabrication due to electrostatic attraction between the drug and the polymer. It was shown that the loading of the Dox during the hexane washing step had the maximum payload of 24.1 mg Dox/g PLA at the highest initial loading concentration of 40 mg Dox/g PLA. Thus, the maximum encapsulation efficiency reached was 60.2% (Figure 2-3) [8]. However, it was found that most of the drug was released as soon as the microbubbles were suspended in buffer. Encapsulation by incorporation is the preferred method due to its higher acoustic performance, but this does not give a high enough drug loading. In order to increase the loading of the Dox onto the shell, nanoparticles that are loaded with the Dox can be incorporated.

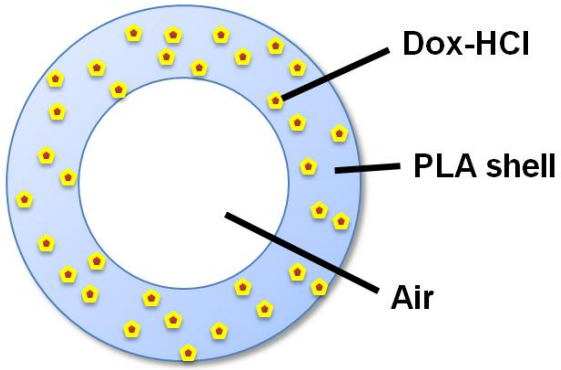

Figure 2-3 Poly (lactic acid) ultrasound contrast agent loaded with hydrophilic doxorubicin

2.5. Nanoparticles

Nanoparticles can be made from a wide variety of organic and inorganic materials such as ceramics, polymers, lipids and metals [36]. To avoid toxicity via accumulation over time, they are required to be biodegradable or easily excreted through the kidneys. However, a recent study showed that nanoparticles that get coated by the patients' serum protein via adsorption, preventing renal excretion, can be coated with zwitterionic or neutral organic coatings to prevent this adsorption [37]. This resulted in final hydrodynamic diameter of less than 5.5 nm in the body, resulting in rapid and efficient urinary excretion. Independent of the microcapsules, nanoparticles can themselves be used as drug delivering agents. This is feasible because they are smaller than the characteristic pore cutoff size in the tumor vasculature, which ranges from 200 nm to 1.2 μm [38]. Nanoparticles can be detected by the reticulo-endothelial system (RES) which can opsonize and clear them away rapidly. In order to increase their half-life in the body, they can be coated with hydrophilic molecules to prevent rapid clearance [39]. There are many different materials that can be used as nanoparticles. Iron oxide nanoparticles would be used in this research.

2.5.1. Magnetic Nanoparticles

Currently, iron oxide nanoparticles are used as contrast agents for X-ray phase computed tomography (SR-PCT) [40] and magnetic resonance imaging (MRI) [41]. MNP improves an MRI scan by producing hypo-intense signaling of the transverse relaxation time (T_2) and the apparent transverse relaxation time (T_2^*).

Intravenous iron oxide particles are superparamagnetic, that is, they retain no magnetic moment in the absence of a field. Saturation magnetization of MNP represents the magnetization that results from the alignment of their magnetic dipoles to the external field. A greater saturation magnetization ensures the localized changes in the longitudinal and transverse relaxation times of the water molecules in the environment to improve the MRI contrast. Since saturation magnetization is also correlated to the size, MNP need to be between 4 to 10 nm to be superparamagnetic [42]. They should also be above 5.5 nm to avoid rapid renal clearance [43]. One way to produce MNP is by a co-precipitation method. Different bases can be used in this method to change the average size of the MNP produced. This ranges from 3.8 nm to 11.5 nm [41]. The size of the MNP correlates to the surface area for the iron oxide-Dox conjugation to occur. In a recent study by Niu, multifunctional microbubbles were designed where Dox loaded PLGA microbubble shells were also loaded with free MNP [44]. The MNP enhanced both ultrasound and magnetic resonance imaging (MRI) of the lymph nodes while targeted chemotherapy is ensured. In other research, the Dox was conjugated to the iron oxide nanoparticles [45]. These work by releasing the Dox in response to the acidic pH of the environment of inner cellular organelles. MNP crystal cores can be capped with a capping agent such as oleic acid which has a molecular weight of 282.46 (Figure 2-4) (Figure 2-5) [46]. The

hydrophilic end of the molecule would be facing the MNP while the hydrophobic end would be unbound. The Dox molecule is expected to be attached to the hydrophobic chains of the oleic acid molecule.

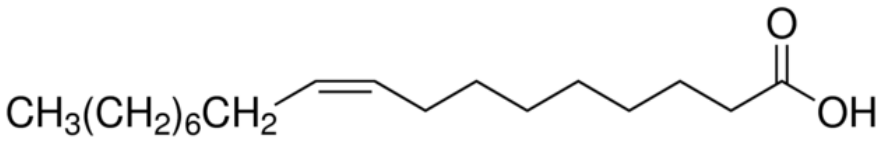

Figure 2-4 Structure of the oleic acid [46]

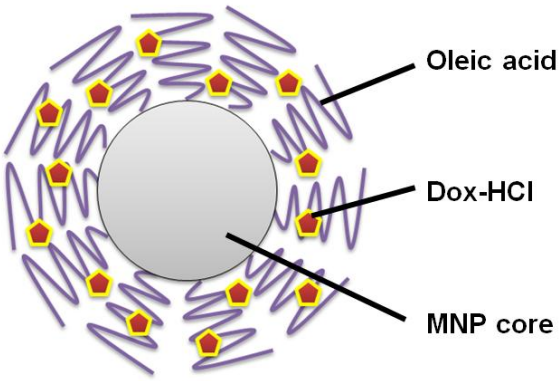

Figure 2-5 Hydrophobic magnetic nanoparticles capped with oleic acid

The oleic acid capped MNP can be further coated with Pluronic F127 to make it hydrophilic (Figure 2-6) (Figure 2-7) [47] [48]. The hydrophobic part of the Pluronic would interact with the hydrophobic part of the oleic acid while the hydrophilic ends of the Pluronic acid would be free floating.

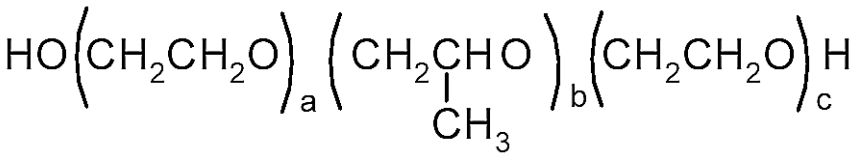

Figure 2-6 Structure of the Pluronic F127 [47]

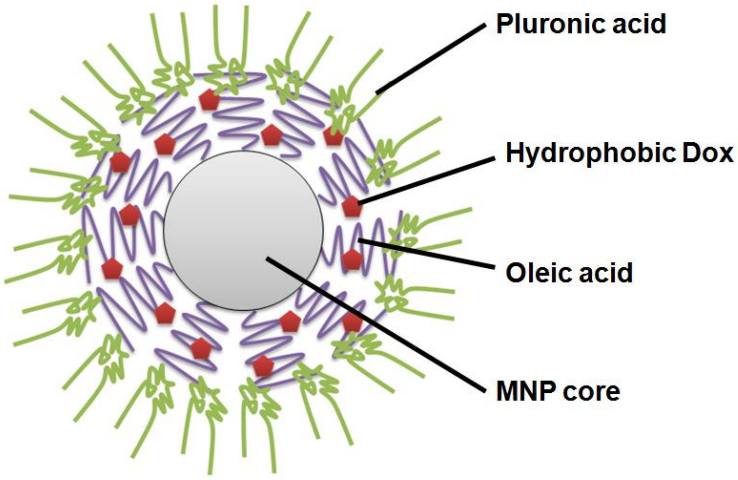

Figure 2-7 Hydrophilic magnetic nanoparticles capped with oleic acid and coated with pluronic acid

3. DESIGN ASPECTS

The criteria and constraints defined for this project ensured that the final targeted chemotherapeutic agent delivering UCA was modified without compromising the acoustic properties. These studies serve as a template for investigations that validate the increased drug loading of the UCA and their ability to be echogenic when used with ultrasound.

The goal is to design PLA UCA that can deliver more of the model chemotherapeutic agent – Dox by first loading it onto MNP to increase the loading surface and then encapsulate these MNP onto the UCA. This must be done without sacrificing their acoustic properties or the size limitations. It would also give another potential mechanism for drug to enter the cell - via endocytosis of the MNP.

Since the UCA resonate under the focused ultrasound, the UCA would only shatter near the tumor cells. The ultrasound can also increase the entry into the cell since the insonation would generate heat in the cell environment, causing the cell membrane to be more permeable to the nanoshards created when the UCA is ruptured.

3.1. Design Constraints and Criteria

Constraints

Microbubbles must have the following properties:

- Microbubbles must be less than 5 μm in diameter to pass through the vascular bed.
- Incorporation of nanocrystals must not compromise the acoustic properties of the microbubble in the area of acoustic enhancement. Enhancement of more than 12 dB during *in vitro* tests has translated to successful *in vivo* imaging.
- Ultrasound irradiation must be responsive within the range of the medical ultrasound.
- The UCA must have at least 15 minute *in vitro* half-life in order to travel through the vasculature of the target tumor at least once when injected into the patient.
- The MNP must be non-toxic and be easily eliminated from the body once it has interacted with the cancer cell.

Criteria

- Final UCA size must be 1-5 μm.
- *In vitro* acoustic enhancement must be ≥ 12 dB.
- Drug loading must be ≥ 6.5 mg Dox/g PLA, the highest achievable dose without nanocrystals.
- In the presence of the ultrasound, the *in vitro* $t_{1/2}$ must be ≥ 15 minutes.

4. SPECIFIC AIMS

The main goal of this research is to increase the loading of the drug Dox in a PLA UCA developed in Wheatley lab, for greater treatment efficiency in cancer. This increased loading will be achieved by co-encapsulating nanocrystals (MNP) that are ligated to the drug as the means to increase the loading and supplement encapsulated Dox in the PLA shell. In addition, MNP could act as magnetic resonance imaging (MRI) contrast agents and X-ray phase computed tomography (SR-PCT) [40].

Aim 1: To develop and characterize PLA UCA which are loaded with MNP.

- Assess the effect of loading MNP on the acoustic properties of UCA. This would ensure that the incorporation of the MNP do not affect the acoustic and drug delivery properties of the PLA microbubbles. Dose and time acoustic response curves were constructed for UCA loaded with MNP.
- Determine the largest loading MNP possible without significantly decreasing the echogenicity.

Aim 2: To develop and characterize MNP conjugated with Dox.

- Determine the highest drug payload possible on the MNP using different MNP capping agents. The method that achieves the highest yield of drug/particle will be chosen for specific aim 3.

Aim 3: To increase the loading of the Dox into the shell of the UCA.

- Determine the mass of Dox that was actually loaded on the UCA with and without the use of the different MNP.
- Modify the UCA fabrication process or the drug formulation to further increase the drug loading.
- Perform acoustic tests to determine echogenicity after loading.

5. MATERIALS AND METHODS

5.1. Materials

5.1.1. Magnetic Nanoparticles

Fe(III) chloride hexahydrate (lot# MKBH8430V) from Sigma-Aldrich (St. Louis, MO), Fe(II) chloride tetrahydrate (lot# BCBH6730V) from Sigma-Aldrich (St. Louis, MO), oleic acid (lot#MKBH5625V) from Aldrich (St. Louis, MO), 1N ammonium hydroxide (lot# 1353221) from Fluka (Pittsburgh, PA), and Pluronic® F-127 (lot# SLBG6026V) from Sigma (St. Louis, MO) were used.

5.1.2. Ultrasound Contrast Agent Polymers and Drug

Poly (lactic acid) (PLA) 100 DL 7E = 115 kDa (lot# LY00414-119) from Evonik Industries (Birmingham, AL), ammonium carbonate (lot#124326) from Fisher Scientific (Fair Lawn, NJ), poly (vinyl alcohol) (MW = 25 kDa, 88 mol% hydrolyzed) (lot# 652279) from Polysciences (Warrington, PA), isopropyl alcohol (IPA) (lot#B0522292) from Acros (New Jersey, NJ), methylene chloride (lot#135806), and hexanes (lot#110593) from Fisher Scientific (Waltham, MA), camphor (lot# 082K2515), chloroform (lot# SHBB7668V), dimethyl sulfoxide (DMSO) (lot#SHBC2572V) and triethylamine (TEA) (lot# 128K1103) from Sigma-Aldrich (St. Louis, MO) and Doxorubicin HCl (lot# 20130702), (lot# A0325A) from Tecoland, (lot# 1000461729) from Fluka (Pittsburgh, PA) were used.

All materials were used as received.

5.2. Methods

5.2.1. Magnetic Nanoparticles Fabrication

5.2.1.1. Fabrication of Oleic Acid Capped Magnetic Nanoparticles [48]

A solution of 11.6 g of $FeCl_3.6H_2O$ and 4.3 g of $FeCl_2.4H_2O$ dissolved in 400 mL of deionized water was continuously purged with nitrogen gas and stirred at 90˚C. After dissolution, 15 mL of NH_4OH was added, followed by a dropwise addition of 9 mL of oleic acid. The black magnetic gel was precipitated and decanted. The gel was washed twice with acetone by sonication in an ice bath using a 0.5-inch probe horn (CL4 tapped horn probe with 0.5″ tip, Misonix Inc., Farmingdale, NY) with a Misonix probe sonicator at 110 W for 30 seconds which is made up of 10 pulses of 3 seconds, separated by 1 second each. The gel was reweighed to get yield mass and mixed with 10 mL of methylene chloride.

5.2.1.2. Fabrication of Pluronic Coated Oleic Acid Capped Magnetic Nanoparticles [49]

Solutions of 0.1 M $FeCl_3.6H_2O$ (811 mg dissolved in 30 mL deionized water) and 0.1 M $FeCl_2.4H_2O$ (298 mg dissolved in 15 mL deionized water) were mixed under nitrogen gas for 5 min. 15 mL of 1 M ammonia solution was added dropwise over 1 min. It was stirred for an additional 20 min. An aliquot of 115.8 uL oleic acid was added and stirred at 80˚C for 30 min. It was then cooled to room temperature. Pluronic acid (100 mg) was added and stirred overnight. The samples were washed with deionized water and then the MNP were collected with a magnet. The samples were ultracentrifuged using 4 tubes of the 38 mL size in the Sorvall WX Ultra Series 80 ultracentrifuge (AH629, Thermo Electron Corporation) at 20000 rpm (72k g-force) for 30min at 10˚C. The MNP

were redispersed in 15 mL water and sonicated. The samples were ultracentrifuged at 20000 rpm for 30 min at 10˚C. It was washed 3 times with deionized water. The MNP were redispersed in 15 mL water and sonicated in an ice bath using the Misonix probe sonicator at 110 W for 150 seconds which is made up of 10 pulses of 3 seconds on, separated by 1 second off each. It was ultracentrifuged at 1000 rpm (180 g-force) for 20 min at 10˚ C to remove large aggregates. The samples were lyophilized in pre-weighed 50 mL centrifuge tubes on a Virtis Benchtop freeze-dryer (Gardiner, NY) -76.5° C (in the vacuum drier chamber) and 17-20 μBar.

5.2.2. Hydrophobic Doxorubicin Formulation [50]

To a solution of 50 mg Dox-HCl dissolved in 100 mL water, 400 uL of Triethylamine was added. Approximately 800 mL of chloroform was used to extract the Dox-base from the water. Using a Buchi Rotavapor RE111 rotary evaporator at 60˚ C, the chloroform was separated from the h-Dox until approximately 10 mL was left. The h-Dox was transferred into a preweighed glass vial and was evaporated to determine the mass of the h-Dox formed. The percentage yield was calculated using the following equation:

$$\%Yield = \frac{Final\ \ Dox\ Weight}{Initial\ \ Dox\ Weight} \times 100 \qquad \text{Eq. 3}$$

There exists a small difference between molecular weight of Dox-HCl of 579.98 and h-Dox of 543.52. However it was ignored for simplicity, and in line with the accuracy by which Dox and Dox.HCl could be measured.

5.2.3. Loading of Doxorubicin onto Magnetic Nanoparticles [48]

The Dox-MNP were freeze dried in water as described above. A mixture of 2 mL of the 12.5% v/v methanol/chloroform was added to 2 mg of the Dox conjugated MNP and shaken overnight. MNP were separated from the solution using neodymium magnets (Grade N52 CMS). After separation of the MNP, 1.5 mL of the remaining clear solution was removed and dried out in a preweighed tube. To determine the Dox loading, 1.5 mL DMSO was added to remove the Dox and was read in triplicates on the Tecan fluorimeter (Männedorf, Switzerland) plate reader at excitation 485 nm, and emission at 591 nm for the h-Dox.

5.2.4. Magnetic Behavior of MNP Loaded with h-Dox:Vibrating Sample Magnetometer

Magnetization of MNP-OA samples with and without Dox loading was measured at 300 K where samples were placed in a uniform magnetic field and sinusoidal physical vibrations were applied. The voltage induced by the MNP was picked up by the coils. The magnetization was recorded for the field between -4000 Oe to 4000 Oe at 100 Oe intervals. Eun Ju Moon from the Materials Department performed this Vibrating Sample Magnetometer VSM test.

5.2.5. Fabrication of Drug or Nanoparticle Loaded Ultrasound Contrast Agents

The following fabrication method was developed by Dalia El Sherif and modified by Kelleny Oum [51] [52]. Poly (lactic acid) UCA was made using the double emulsion technique (w/o/w). At room temperature, 500 mg of PLA and 50 mg of camphor were dissolved in 10 mL of methylene chloride, covered with aluminium foil and stirred in a 50 mL beaker. In another small beaker, 400 mg of ammonium carbonate was dissolved in 10 mL of DI water. The loading of the drug or the nanoparticles depend on their hydrophilic behavior; when it is hydrophobic, it is added to the methylene chloride mixture, otherwise, it is added to the ammonium carbonate mixture. After dissolution, 1 mL of the ammonium carbonate solution was added to the polymer mixture and it was sonicated in an ice bath using Misonix probe sonicator at 110 W for 30 seconds which is made up of 10 pulses of 3 seconds on, separated by 1 second off each. The sonicated solution was added to 50 mL of cold (4^{o} C) 5% poly vinyl alcohol (PVA) in a 500 mL beaker. Thereafter, it was homogenized with a Brinkmann PT 3100 homogenizer with a Polytron PT-DA 3020/2 generator for 5 min at (2000 g-force, 9.6k rpm). Then 100 mL of 2% v/v isopropyl alcohol (IPA) was added to the homogenized mixture and the top was partially covered with parafilm. The mixture was stirred on a magnetic stir plate for 1.5 hour at 375 rpm to evaporate the methylene chloride. The mixture was poured into 4 tubes of 50 mL maximum volume tubes and centrifuged using Beckman Coulter, Allegra^{TM} 21 centrifuge at 5000 rpm (2.6k g-force) for 5 min. The supernatant was discarded while the microbubbles were combined into one tube before re-centrifuging them for 5 min at 5000 rpm. The supernatant was discarded and the microbubbles were gently washed with hexane three times. The remaining hexane from the microbubbles

was allowed to evaporate in the chemical fume hood for 30 min. DI water was added and the mixture was re-centrifuged for 5 min at 5000 rpm (2.6k g-force). The supernatant was discarded. The tube was covered with a Kim wipe and an elastic band before flash freezing the microbubbles in liquid nitrogen. The frozen microbubbles were put into the Vitris Benchtop freeze dryer (Gardiner, NY) for 72 hours in order for water, ammonium carbonate and camphor to sublime.

5.2.6. Characterization of the Ultrasound Contrast Agents

5.2.6.1. Zeta potential and Size of the Ultrasound Contrast Agent

Using the Malven's Zetasizer nano ZS (Worcestershire, UK) and DTS Nano software, the following tests were performed. 1 mg of the fabricated sample was suspended in 1 mL PBS and tested in DTS0012 for size determination and Polydispersity Index (PDI). Similarly, 1 mg of fabricated sample was suspended in DI water in a Malvern zeta capillary cuvette DTS1060 for the zeta potential testing in the Zetasizer. The samples were measured in triplicate and particle sizes were reported as peak % number.

5.2.6.2. Cumulative Dose Response: contrast enhancement as a function of ultrasound contrast agent dosage

The test system consisted of one directional pulsed A-mode ultrasound system with a single element, broadband, 12.7 mm element diameter, 50.8 mm spherically focused transducer with center frequency of 5 MHz with a -6 dB bandwidth of 92% as shown in Figure 5-1. A sample vessel containing 50 mL of the phosphate buffered saline (PBS at pH 7.4) was settled inside the deionized water bath at 37° C. The oscilloscope

was turned on and the pulser/receiver (model 5072 PR, Panametrics, Inc., Waltham, MA) that sends pulses to the transducer at a repetition frequency (PRF) of 100 Hz was focused though an acoustic window on the sample vessel using an x-y positioning system (Edmund Scientific, Barrington, NJ). The received signals was amplified by 40 dB and delivered to the digital oscilloscope (Lecroy 9350A, Lecroy, Chestnut Ridge, NY). 800 μL of the PBS was removed from the sample vessel and was added to the 3 mg of the microbubbles. It was vortexed for 30 seconds until all the microbubbles were suspended evenly. A 20 μL sample of the microbubble mixture was added to the sample vessel every minute which was repeated 10 times. The LabView Main Ultrasound Program was used to collect data times to create a cumulative dose response curve.

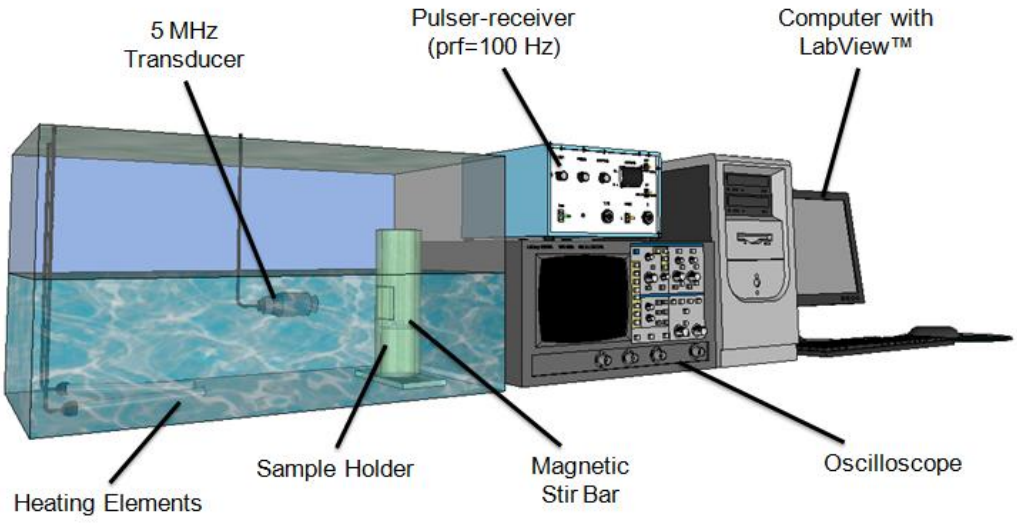

Figure 5-1 Schematic of the in vitro acoustic testing set-up, image courtesy of Tarn Teraphongphom

5.2.6.3. Time Response: stability of the agent during continuous insonation

A sample vessel containing 50 mL of PBS at pH 7.4 was placed inside the water bath. The oscilloscope and the pulser/receiver were turned on and the transducer was focused on the sample vessel using the x-y positioning system. A dose that was within the linear part of the dose response curve was added to the PBS and was insonated continuously with a PRF of 100 Hz and a peak negative pressure amplitude of 0.45 MPa (energy 1) and 0.94 MPa (energy 4) [53]. The LabView Main Ultrasound Program was used to collect the data.

5.2.6.4. Scanning Electron Microscopy

Environmental scanning electron microscope (SEM) (FEI XL30, Hillsboro, OR) was used to take images of UCA. Around 1 mg of the lyophilized UCA was gently fixed on a carbon tape and using a Denton Desk-II sputtering system (Denton Corp, NJ), the sample was sputter-coated with platinum for 3 seconds. Images of the samples at various magnifications was taken at accelerating voltage of 5 kV and a spot size was 3. All sputter coating and SEM imaging were performed in the Drexel University Central Research Facility by Wheatley Lab's designated SEM imaging personnel, Lauren Jablonowski. These images were used to determine the morphology of the fabricated samples.

5.2.7. Doxorubicin Loading

Approximately 2 mg of fabricated Dox containing PLA microbubbles was added to 2 mL DMSO and vortexed for 30 seconds until the polymer had dissolved. A Tecan fluorimeter (Männedorf, Switzerland) was used to read the fluorescence of the mixture at

an excitation wavelength of 495 nm and an emission wavelength of 585 nm for the hydrophilic Dox and excitation wavelength of 485 nm and an emission wavelength of 591 nm for the h-Dox. These excitation and emission wavelengths for the h-Dox were determined using the fluorescence scans. All samples were read in triplicate. Doxorubicin concentrations were calculated based on standard curves of known amounts of Dox in DMSO. The loading and encapsulation of the Dox on the UCA were determined using Eq. 4 and Eq. 5.

$$\%Loading = \frac{Final\ \ Dox\,Weight}{Total\ \ UCA\,Weight} \times 100 \qquad \text{Eq. 4}$$

$$\%Encapsulation Efficiency\ = \frac{Final\ \ Dox\,Weight}{Initial\ \ Dox\,Weight} \times 100 \qquad \text{Eq. 5}$$

5.3. Statistical Methods

Statistically significant differences between multiple groups were determined using one-way analysis of variance (ANOVA) and multi-compare function using MATLAB. Statistical significance was determined using 95% confidence interval (p=0.05). Error bars were displayed as standard error about the mean (SEAM).

6. RESULTS AND DISCUSSION

The main goal of this research was to create PLA UCA that would have increased Dox payload in order to improve patient treatment. The systemic side effects of the Dox could be decreased while increasing safety since there would be a reduction in the dose of drug administered. This goal was hypothesized to be possible through increasing the surface area of the PLA UCA on which the Dox can be entrapped as well as increasing Dox's affinity to be encapsulated.

Magnetic nanoparticles capped with oleic acid were synthesized in the first phase of the experiment. The effects on the structure and acoustic properties of the UCA as a result of increasing the MNP-OP loading in UCA were tested. These samples were made immediately after the fabrication of the MNP-OA. Magnetic nanoparticles capped with oleic acid were observed to be unstable and sink in the methylene chloride solution after one week of synthesis which resulted from losing their capping agent. Ultrasound contrast agents made from these were found to be non echogenic. Therefore, another method of synthesis was investigated to create magnetic nanoparticles capped with oleic acid. They were further coated with Pluronic acid. During the second phase of the experiment, the Dox payload and entrapment efficiency of MNP-OA-PA were tested. Microbubbles loaded with various amounts of MNP-OA-PA were also fabricated and tested for their acoustic properties. Samples of h-Dox were made and encapsulated in UCA to determine whether the resulting payload of Dox would be increased by using the hydrophobic form. The tests to compare the structure and acoustic properties of these h-Dox loaded UCA to that of the hydrophilic Dox were also performed.

Aim 1 – Loading of Magnetic Nanoparticles on Ultrasound Contrast Agents

The co-precipitation method of synthesizing MNP-OA yielded 503±34 mg with a yield percent of 63.32%. These were encapsulated in PLA UCA by adding them in the methylene chloride along with the PLA during the fabrication process. 33 wt% MNP-OA encapsulated UCA had 250 mg loaded onto them while the 50 wt% MNP-OA encapsulated UCA had 500 mg loading. Apart from the aforementioned loadings, the fabrication method was the same as the unloaded UCA which were used as controls in the following tests.

6.1.1. Acoustic Properties of MNP-OA Loaded UCA

The effect of MNP-OA loading in the PLA-UCA on the *in vitro* acoustic properties were tested using the set up shown in Figure 5-1. Figure 6-1 shows the *in vitro* enhancement of the various loadings of the MNP-OA compared to the unloaded UCA, the control.

The maximum enhancement of the unloaded sample was at 18.81±0.52 dB at the 6.12 μg/mL dose. Thereafter, the acoustic enhancement decreased to 16.89 dB at the 15.30 μg/mL dose due to shadowing. Shadowing is caused by the inability of ultrasound waves to pass through a dense concentration of UCA and the inability for the backscatter from the UCA to reach the transducer due to it being reflected continuously between the focal point and the transducer [54-55]. The hindrance was increased with dose.

Similar shadowing pattern are seen in the dose response curve of the 33 wt% MNP-OA loaded UCA which reached the highest acoustic enhancement of 14.77±0.61 dB at 6.12 μg/mL dose level. This acoustic enhancement is significantly lower than the control UCA ($p<0.0001$). The overall dose dependent acoustic enhancement of the 50

wt% MNP-OA loaded UCA was also significantly lower than the unloaded which has the maximum of 12.73±0.80 dB, read at a high dose of 15.3 µg/mL ($p<0.0001$). This was also lower than the 33 wt% MNP-OA UCA ($p<0.05$). No shadowing effect was seen in 50 wt% MNP-OA loaded UCA. There was no statistically significant difference in acoustic enhancement between the two MNP-OA loaded UCA at 15.3µg/mL.

These results suggest that loading the MNP-OA shows decreased acoustic enhancement by the UCA. The absence of the shadowing effect by the 50 wt% MNP-OA when compared to the 33 wt% MNP-OA could be due to fewer acoustically active microbubbles per dose. Addition of the MNP-OA onto the UCA can successfully result in acoustic enhancements over the acceptable enhancement of 14 dB.

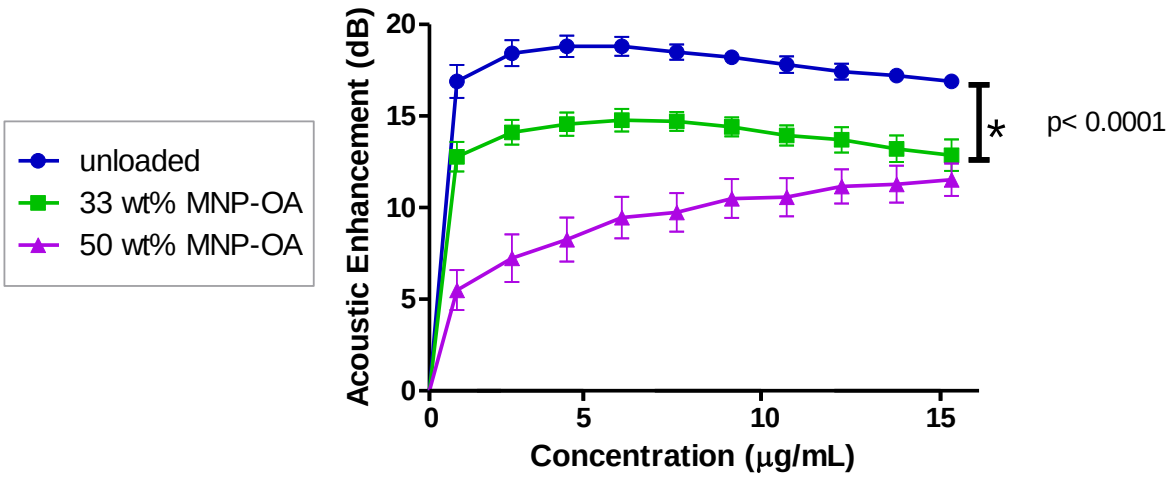

Figure 6-1 The effect of varying MNP capped with oleic acid loading on the acoustic enhancement of UCA (n=3, error bars=SEAM)

The stability of the MNP-OA loaded UCA when subjected to *in vitro* ultrasound was also tested as shown in Figure 6-2. All three samples had some degree of loss of enhancement within 15 minutes of subjecting the UCA to ultrasound but their half lives

were all more than 15 minutes. 50 wt% MNP-OA stability decreased over time, however, 33 wt% MNP-OA loaded UCA showed that they can be significantly more stable when compared to the blank UCA (p=0.0029). As seen with the 33 wt% MNP-OA, adding some MNP-OA can strengthen the shell of the UCA, enabling them to withstand the forces exerted by the ultrasound longer.

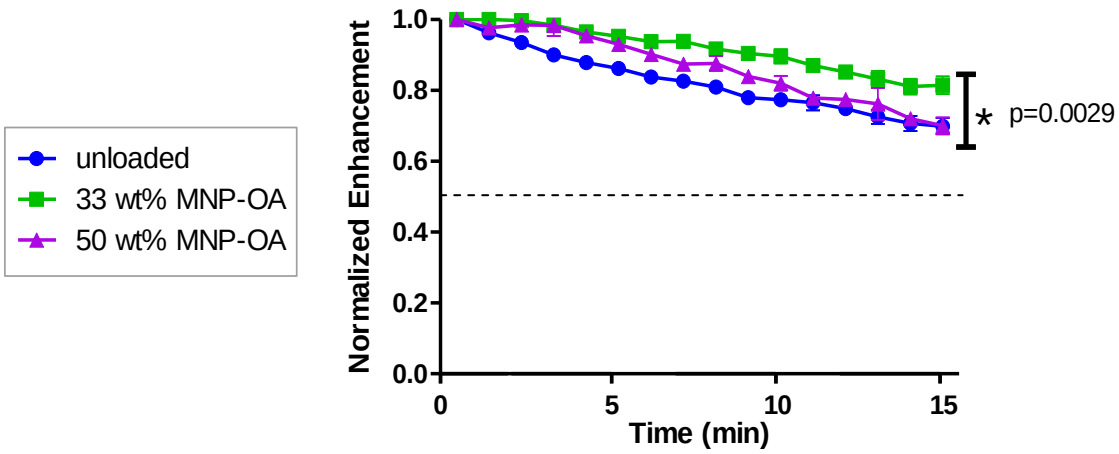

Figure 6-2 The effect of varying MNP capped with oleic acid loading on the stability of the UCA (n=3, error bars=SEAM)

From the two different loadings of MNP-OA, 33 wt% MNP-OA had better acoustic properties; both acoustic enhancement and stability were higher than that of 50 wt% MNP-OA when subjected to ultrasound.

6.1.2. Size and Surface Properties of the MNP-OA Loaded UCA

No statistically significant differences were seen among the 3 samples in terms of size as shown in Figure 6-3 ($p>0.05$). Loading MNP-OA onto the UCA did not affect the size of the fabricated UCA since the size of the 33 wt% MNP-OA and 50 wt% MNP-OA were 1847±227 nm and 2213±390 nm. The unloaded sample was 2044±78 nm. Therefore, size was not a factor that can explain the differences seen in the acoustic enhancement and stability of the loaded UCA.

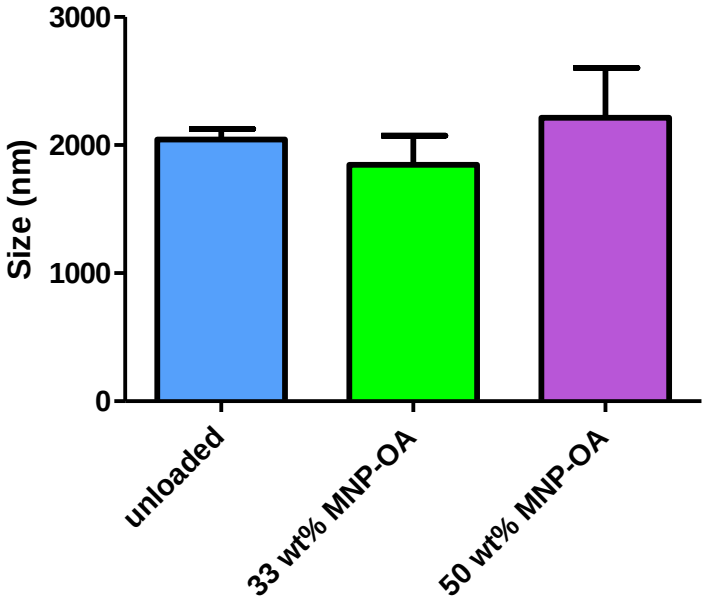

Figure 6-3 The effect of varying the loading mass of MNP capped with oleic acid on the size of UCA (n=3 except 50 wt% MNP-OA, n=2, error bars=SEAM)

The 33 wt% MNP-OA had a PDI of (0.270±0.020). Only the unloaded (0.212±0.027) and the 50 wt% MNP-OA (0.307±0.024) were statistically different from each other in terms of PDI ($p=0.0336$) (Figure 6-4). The 50 wt% MNP-OA was the most poly dispersed sample and this could mean that some of the mass in the final lyophilized

product may not be hollow UCA that are echogenic but small solid particles. However, all samples had a polydispersity index less than 0.7; a value above which samples are considered to have a broad size distribution.

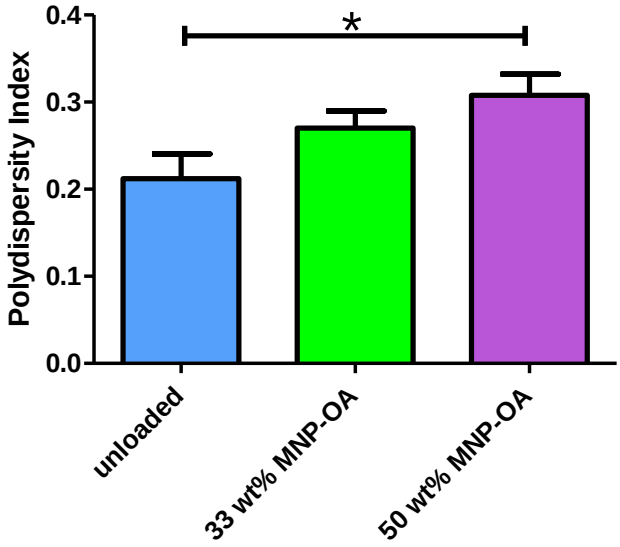

Figure 6-4 The effect of varying the loading mass of MNP capped with oleic acid on the polydispersity of the UCA made (n=3, error bars=SEAM)

SEM images shown in Figure 6-5 showed more evidence of the presence of small spherical particles fabricated in the MNP-OA loaded UCA. Since they are small, it could be possible that there is no gas core within them. Since these were present in each dose that was added to the sample vessel, the acoustic enhancements were lower overall for the loaded particles. There were more wrinkled and poorly formed particles present in the 50 wt% MNP-OA loaded UCA compared to the 33 wt% MNP-OA, which may also explain the lower acoustic enhancements of the 50 wt% MNP-OA loaded UCA. It may seem that the particles in B and C of Figure 6-5 do not reflect the size measurements shown in Figure 6-3. However, the size results are not the average size of the sample but the size at which most of the particles were formed.

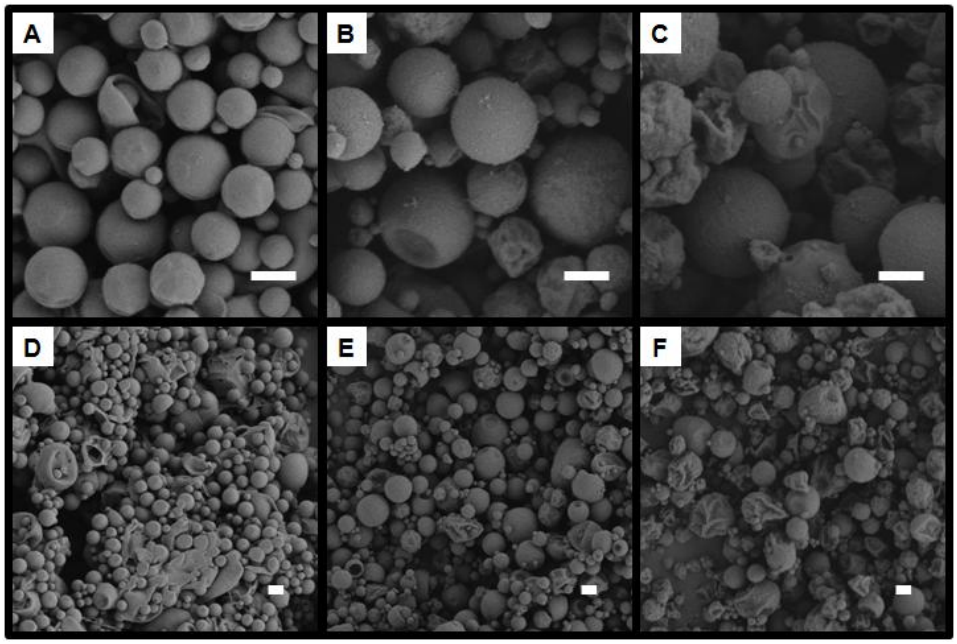

Figure 6-5 SEM images comparing the morphology of the UCA loaded with MNP capped with oleic acid. Top row has magnification of 10 000x while the bottom row is at 3000x. All size bars are 1um. Image (A) unloaded control UCA (B) 33wt% MNP-OA (C) 50wt% MNP-OA (D) unloaded control UCA (E) 33 wt% MNP-OA (F) 50 wt% MNP-OA

The charge on the three groups as measured by zeta potential was significantly different from each other ($p<0.05$) (Figure 6-6). The controls had a significantly more negative charge (-29.35±1.02 mV) when compared to the 50 wt% MNP-OA loaded UCA. The zeta potential values for 33 wt% and 50 wt% MNP-OA loading was -25.83±1.35 mV and -14.25±0.93 mV. Since 50 wt% MNP-OA was of more positive zeta potential, it could clamp together when injected into the patient. The oleic acid capping makes the MNP hydrophobic, thus causing an increase in the zeta potential of the MNP-OA loaded UCA. This could suggest the presence of MNP-OA on the surface of the PLA shell and that MNP-OA was not present only inside the shell or the core of the UCA. This could further explain the appearance of a rough surface on the spherical UCA seen in Figure 6-

5 (B) 33 wt% MNP-OA and (C) 50 wt% MNP-OA at 10 000x magnification when compared to (A) the unloaded control sample.

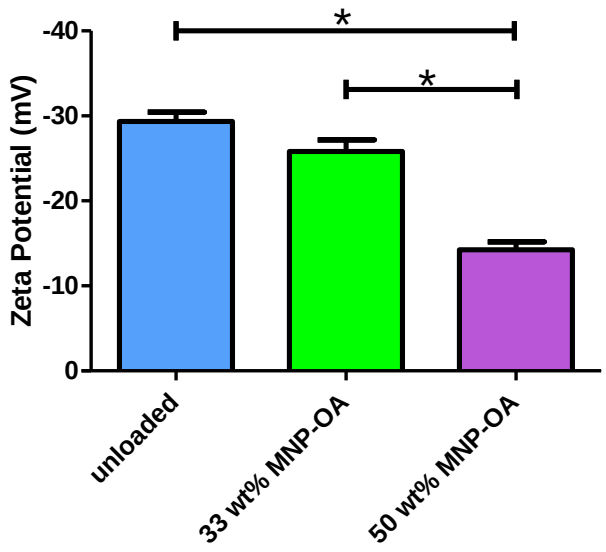

Figure 6-6 The effect of varying the loading mass of the MNP capped with oleic acid on the zeta potential of the UCA (n=3, error bars=SEAM)

6.1.3. Storage behavior of MNP-OA

The MNP-OA which had been synthesized were dispersed in methylene chloride and were stored in the 4˚ C refrigerator. It was observed that after one week, the magnetic nanoparticles would settle to the bottom of the vial. Any bubbles made from these were found to be non echogenic (n=3). The capping agents, oleic acids, may disperse over time in the methylene chloride, causing the magnetic nanoparticles to be attracted to each other and clump together. The previous design was modified to ensure that the magnetic nanoparticles did not lose their capping agents to the methylene chloride solution, since these are vital in entrapping the Dox to the MNP.

Aim 2 – Entrapment of Doxorubicin onto Magnetic Nanoparticles

Magnetic nanoparticles which are capped with the oleic acid were further coated with Pluronic acid so that the oleic acid would not be dispersed into solution, but instead surround the magnetic nanocrystals. Figure 2-7 shows the proposed design of this nanoparticle design. The entrapment and unloading method used by Jain et al was closely followed [49]. Firstly, the hydrophilic Dox was converted to its base form using TEA by a procedure described by Kwon [50]. When TEA was added to the Dox in aqueous solution, it changed the color from red to purple. The h-Dox base was extracted from the salts using chloroform, which gradually developed a dark orange color. The chloroform containing the Dox base was collected and evaporated off using the rotary evaporator to form a dark red solution. The remaining chloroform was left to be evaporated off for 4 days in the chemical hood to ensure that as much chloroform as possible was removed. The yield was used to calculate the ratio of h-Dox made when compared to the amount of Dox-HCl that was initially used. Assuming that h-Dox is made from the reaction between TEA and Dox-HCl, the concentration of the Dox-HCl that was left in the water after the extraction with chloroform was determined. Figure 10-1 found in the Appendix section shows the standard curve that was used to determine the mass of the Dox-HCl left behind in the water. 98.84 % yield was found (n=1). The amount of Dox loaded on to the MNP when 1 mg of h-Dox was loaded onto 10 mg of MNP-OA-PA was determined using the following standard curve found in Figure 10-1. It was found that 0.288 mg h-Dox was loaded on each 1 mg of MNP-OA-PA (n=1). A vibrating magnetometer was used to determine whether magnetization of the MNP-OA-PA was affected by the loading of the h-Dox and the results are shown in Figure 6-7. There was no change in the overall

magnetization which indicates that the Dox is not interacting directly to the magnetic crystal core.

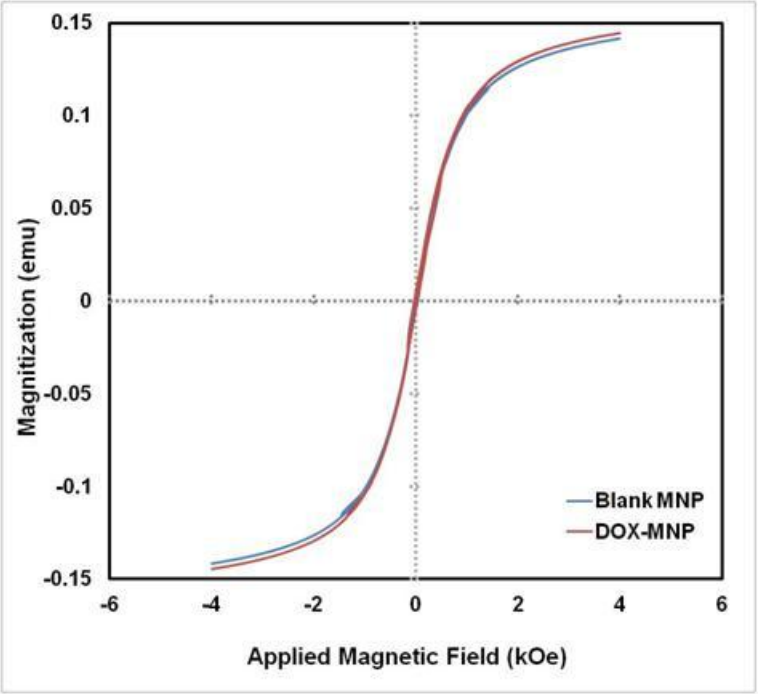

Figure 6-7 Comparison in magnetization with and without loading h-Dox on MNP capped with oleic acid and coated with pluronic acid. It was measured at 300 K at room temperature

6.2.1. Characterization of MNP-OA-PA loaded UCA

While the h-Dox loading onto the magnetic nanoparticles was carried out in the previous section, the loading of the new MNP-OA-PA onto the UCA was being tested. Since the MNP-OA loaded UCA were found to be non echogenic when 1 week old MNP-OA particles were used, Pluronic acid coated MNP-OA were loaded onto the UCA to determine whether the acoustic properties were as similar to when they were not coated with pluronic acid.

Contrast agents were prepared loaded with 26 mg, 56 mg and 250 mg of MNP-OA-PA, which correspond to 5 wt%, 10 wt% and 33 wt% of the overall UCA. The acoustic enhancement of all the MNP-OA-PA loaded samples was found to be lower than 6 dB, equivalent to baseline. In an attempt to identify the cause of this, UCA agents were loaded with 54 mg pluronic acid (10 wt% pluronic acid UCA). This loading mass was determined by the ratio of pluronic acid added to the MNP-OA during its fabrication. Using this assumption, 54 mg was the amount of pluronic acid expected to be present in the 250 mg MNP-OA-PA loaded UCA. With the exception of the 26 mg MNP-OA-PA in MeCl, other samples were added to the UCA fabrication process along with the ammonium carbonate dissolved in water since the particles were believed to be hydrophilic. The particles loaded with MNP-OA-PA were relatively similar in size to the unloaded control in Figure 6-8. The Pluronic acid UCA and Dox-PVA-MNP UCA showed smaller UCA formation but they were more dispersed as seen in Figure 6-9.

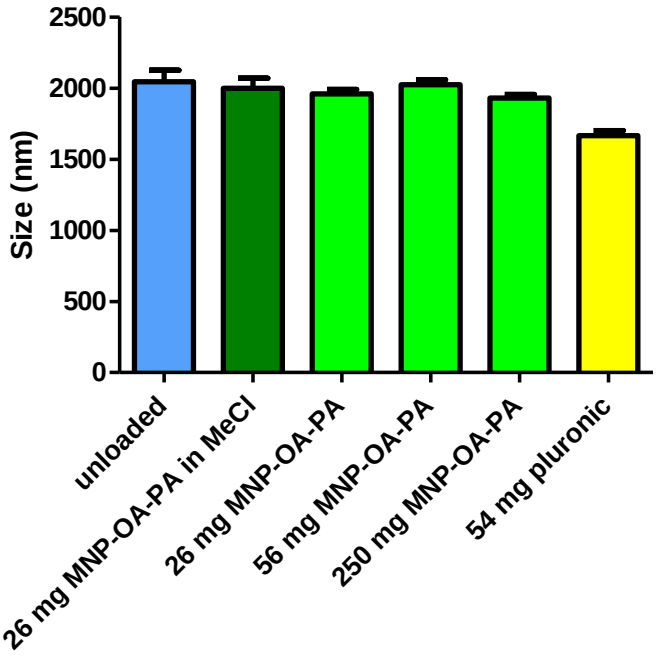

Figure 6-8 The effect of varying the loading mass of MNP capped with various molecules on the size of UCA (n=1, error bars=SEAM)

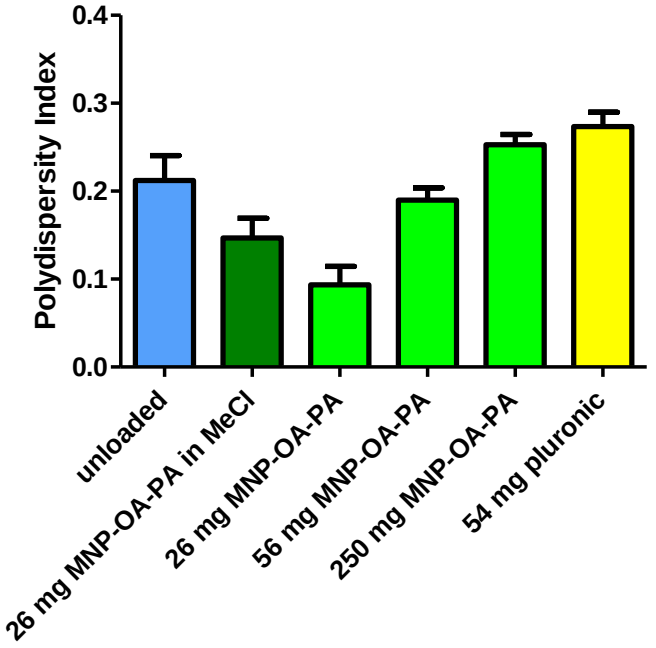

Figure 6-9 The effect of varying the loading mass of MNP capped with various molecules on the polydispersity index of UCA (n=1, error bars=SEAM)

Scanning electron microscope images supported this claim as seen in Figure 6-10. The UCA present were much smaller and there were many unformed UCA present in those with higher Pluronic acid present in the UCA. This could further support the hypothesis that the Pluronic acid may be interacting with the UCA structure. Additional samples to make the n=3 and testing decreasing loadings to the mass of Pluronic acid found in the 5 wt% MNP-OA-PA could make the data conclusive. Decreasing the loading of the MNP-OA-PA decreased the size dispersity in the final UCA made.

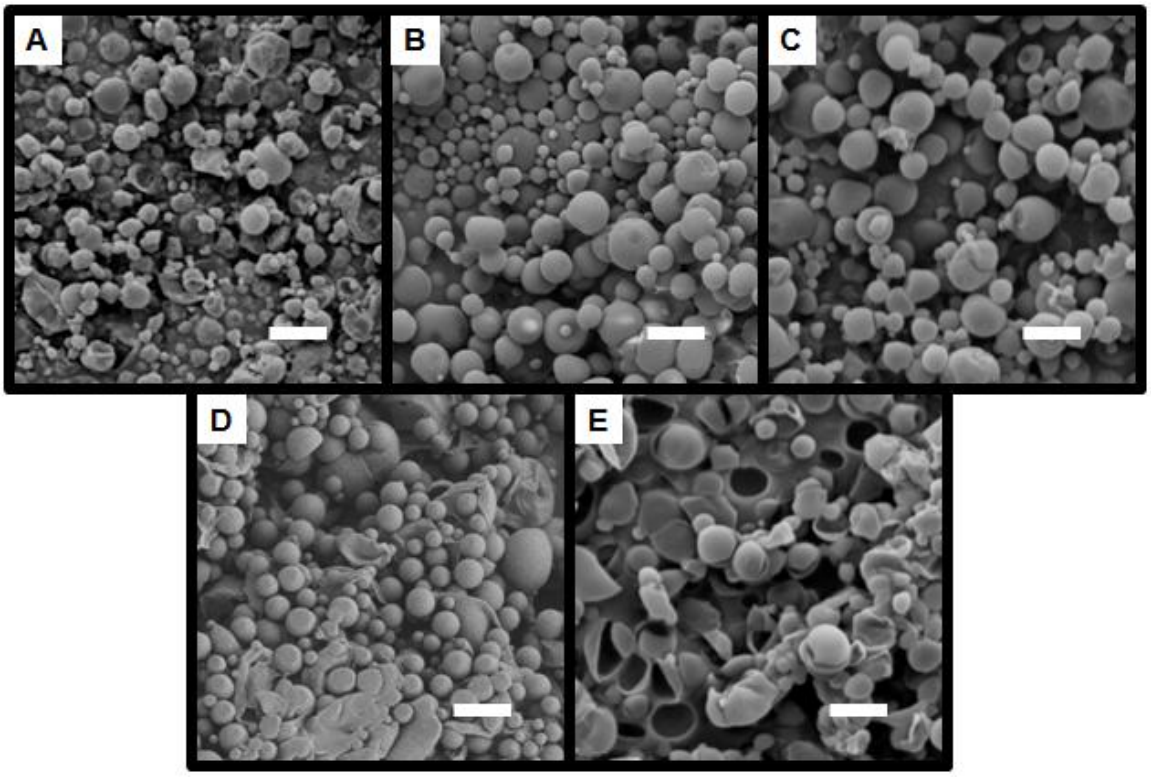

Figure 6-10 SEM images comparing the morphology of the UCA loaded with MNP-OA-PA. Magnification is 3500x. All size bars are 2.5μm. Image (A) 250 mg MNP-OA-PA in Aq (B) 56 mg MNP-OA-PA in Aq (C) 26 mg MNP-OA-PA in Aq (D) blank control UCA (E) 54 mg pluronic acid in Aq

The zeta potentials of the 10 wt% and 33 wt% were not reported due to problems with the zetasizer, but all other samples' data are shown in Figure 6-11. The decreased zeta potential in Pluronic acid loaded UCA when compared to the control and the 26 mg MNP-OA-PA loaded could be due to modifications in the overall charge caused by the presence of hydrophilic ends. Since they were more negative, they would not cause any clamping.

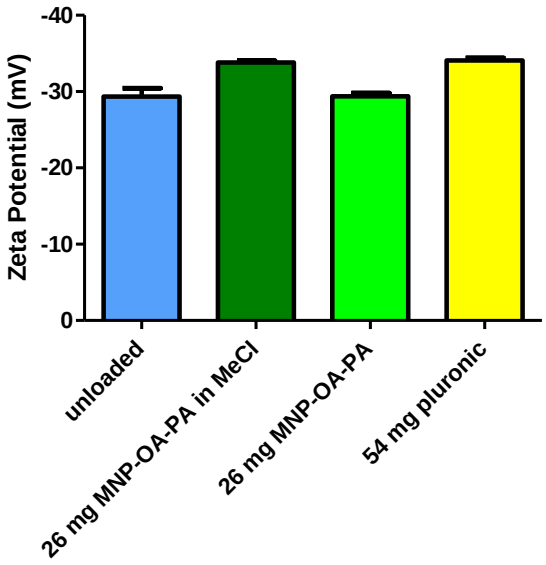

Figure 6-11 The effect of varying the loading mass of MNP capped with various molecules on the zeta potential of UCA (n=1, error bars=SEAM)

Due to the lack of acoustic enhancements seen with UCA loaded with MNP-OA-PA samples, a new type of fabrication methods should be considered. The interference with the acoustic enhancement of the UCA when loaded with the MNP-OA-PA along with low entrapment of the Dox into the nanoparticles, make this strategy to increase the loading of the Dox onto the UCA using MNP a design that requires a much more extensive review than is within the scope of this thesis.

Aim 3 – Increasing Doxorubicin Loading onto Ultrasound Contrast Agents

It was hypothesized that encapsulating the hydrophobic form of the doxorubicin into the PLA UCA would increase the drug encapsulation. This is mainly due to the deprotonation of the glycosidic amino group of the Dox-HCl by the TEA, which make it hydrophobic. Since methylene chloride, also called dichloromethane, is a polar solvent, during the UCA fabrication process, the h-Dox would be more attracted to the methylene chloride rather than the PLA which is uncharged. On the other hand, when it is in its hydrophobic form, the methylene chloride would made it favorable for the less polar Dox to associate with the non polar PLA (Figure 6-12). Also, the papers in which Dox was loaded onto the MNP nanoparticles stabilized by hydrophobic capping agents first converted the Dox-HCl into the Dox base which also supported this direction of the project [48] [56]. In addition, in a previous study by Cochron et al, it was shown that loading a hydrophobic drug paclitaxel onto the shell of the PLA UCA can give a much higher maximum payload of 129.46±1.80 μg paclitaxel/ mg PLA [53]. Thus, altering the formulation of the desired drug into its hydrophobic form would increase loading into the PLA shell.

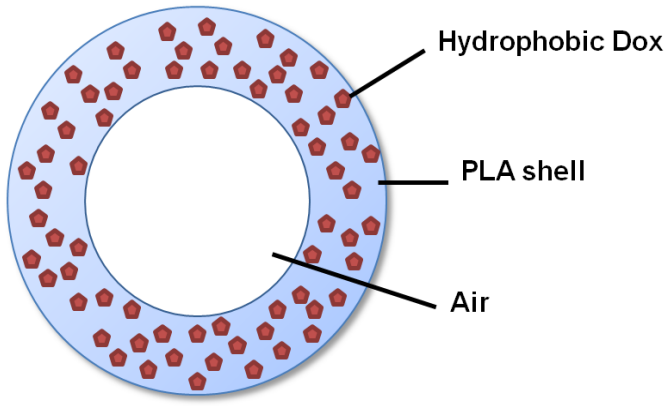

Figure 6-12 Proposed design of the final design where h-Dox was encapsulated into the PLA shell

6.3.1. Doxorubicin Encapsulation

In order to compare the amount of two forms of Dox loaded onto the UCA, 2 different standard curves were made – one for the hydrophilic Dox (Figure 10-2) and one for the h-Dox (Figure 10-3). The fluorescence reading for each was done at their optimum wavelengths on their emission and excitation spectrum scans. The optimum gain attained for the standards were used to read the UCA samples dissolved in DMSO. The 3 wt% hydrophilic Dox loaded UCA which had been chosen in the previous study to have the optimal combination of high acoustic enhancement of 18 dB, tight size distribution of PDI 0.309 and 8 mg Dox/ g PLA was used as a control to which the h-Dox loaded UCA could be compared to results obtained in the previous study [8]. Compared to the 3 wt% hydrophilic Dox loaded UCA which had 9.46±0.28 mg Dox/g PLA, 3 wt% hydrophilic Dox loaded UCA had a significantly higher pay load of 17.75±0.42 mg Dox/g PLA ($p<0.0001$) (Figure 6-13). Doubling the initial loading from 30 mg Dox/g PLA to 60 mg Dox/g PLA significantly increase the payload to 27.18±0.39 mg Dox/g PLA ($p<0.0001$).

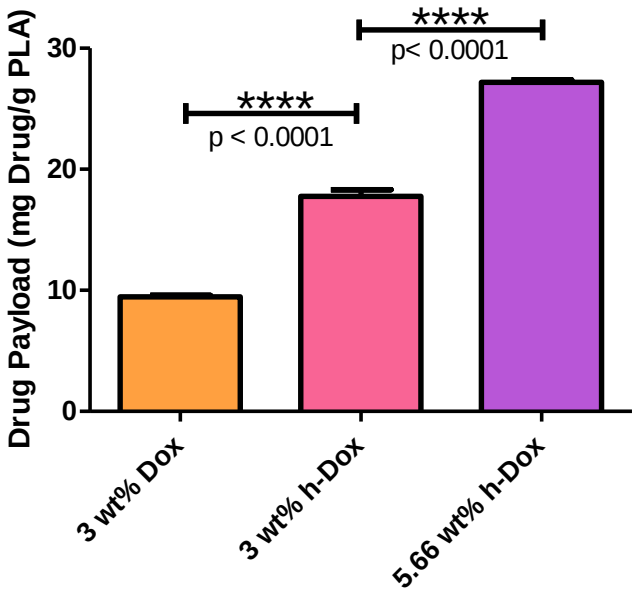

Figure 6-13 The effect of varying the loading of different forms of Dox on the drug payload (n=3, error bars=SEAM) ($p<0.0001$)

The encapsulation efficiency of the 3 wt% h-Dox loaded UCA had a significant increase from 26 % to 51 % when compared to 3 wt% hydrophilic Dox loaded UCA as shown in Figure 6-14. Increasing the loading to 60 mg Dox/g PLA decreased the encapsulation efficiency despite the higher drug payload. The increase in drug encapsulation would allow a higher dose of Dox to be delivered to the tumor with the same amount of agent administered to the patient.

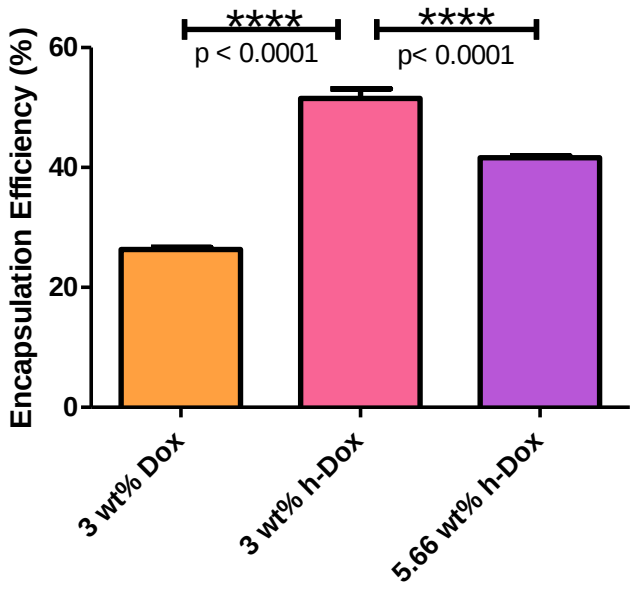

Figure 6-14 The effect of varying the loading of different forms of Dox on the encapsulation efficiency (n=3, error bars=SEAM)

6.3.2. Acoustic Properties of Hydrophobic Dox Loaded UCA

Unloaded microbubbles were used as controls to which the acoustic properties of the Dox loaded UCA could be compared to. The three Dox loaded samples did not have any shadowing affect as did the unloaded UCA (Figure 6-15). The highest acoustic enhancement was at 15.8±2.97 dB at 13.77 μg/mL for the 3 wt% hydrophilic Dox loaded UCA. The highest acoustic enhancement of 12.69±0.81 dB was seen at the largest dose recorded (15.3 μg/mL) for the 3 wt% h-Dox loaded UCA. Acoustic enhancement of the 8.25±0.27 dB was seen at the largest dose recorded (15.3 μg/mL) for 5.66wt% h-Dox loaded UCA. Overall, the 3wt% loadings of the two Dox forms were significantly different from each other, h-Dox UCA being much lower than the hydrophilic ones. Both h-Dox loaded UCA had dose response curves that were still increasing their enhancement with dose at the largest dose recorded, making it possible that higher loading can increase

their acoustic enhancement. Compared to the 3 wt% hydrophilic Dox, the 3 wt% h-Dox had a significantly lower acoustic enhancement ($p<0.05$).

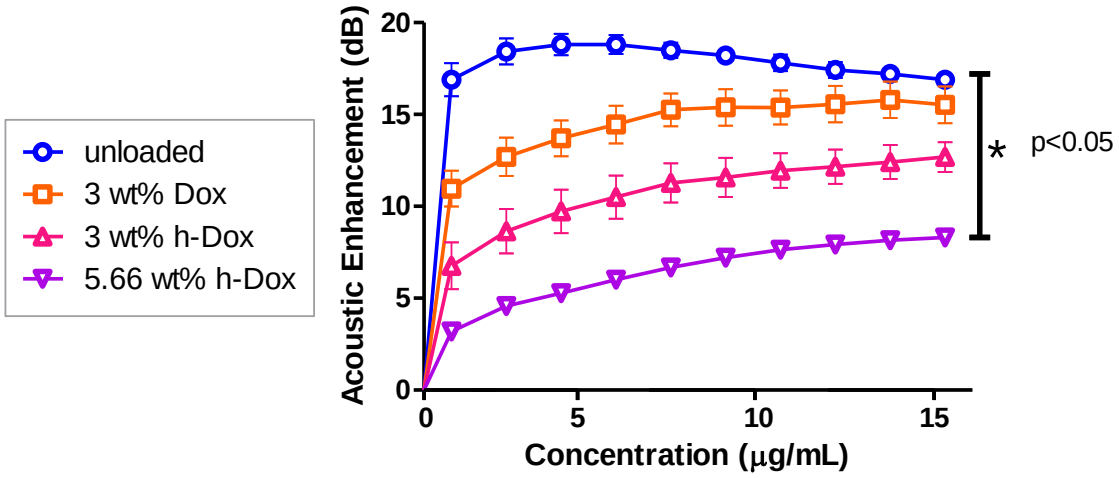

Figure 6-15 The effect of varying the loading of different forms of Dox on the acoustic enhancement of UCA (n=3, error bars=SEAM.

The stability of the Dox loaded bubbles was then tested as shown in Figure 6-16. It was observed that 3 wt% h-Dox was slightly more stable than the unloaded UCA at lower ultrasound energy of 1 and this difference significantly increased at energy 4. The half lives of 3 wt% h-Dox and 5.66 wt% h-Dox were much longer than 15 minutes for energy 1 ultrasound waves. Ultrasound at energy 4 was used to determine whether the UCA could be ruptured by ultrasound since they were seen to be very stable at energy 1. Energy 4 ultrasound were able to decrease the 3 wt% h-Dox to half its initial enhancement at 5 minutes, showing that h-Dox can be ruptured with ultrasound. Moreover, the hydrophilic Dox loaded UCA were less stable and had a half life of around 9 minutes for energy 1. The charge on the hydrophilic Dox could have made the shells,

which are made out of PLA, a hydrophobic compound, to be less stable while the presence of another hydrophobic compound in the shell increased its stability.

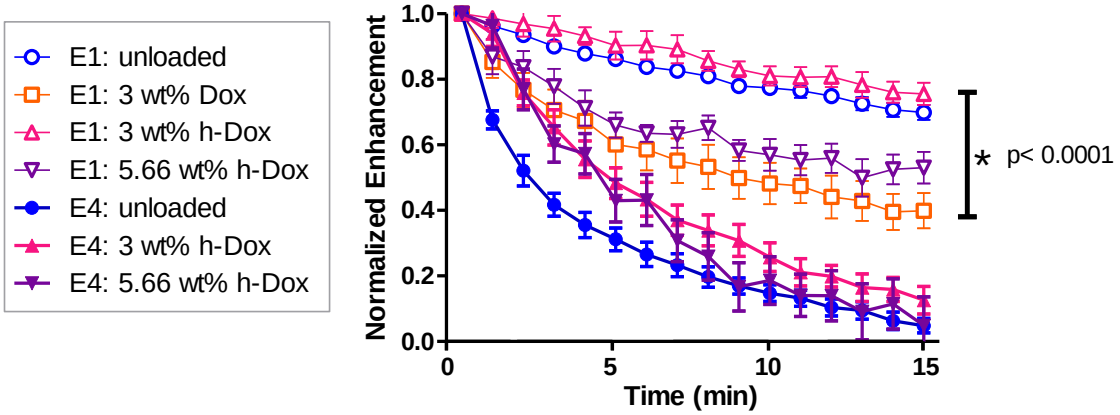

Figure 6-16 The effect of varying the loading of different forms of Dox on the stability of UCA (n=3, error bars=SEAM)

6.3.3. Size and Surface Properties of the Hydrophobic Dox Loaded UCA

The 3 wt% h-Dox loaded UCA had a significant increase in size compared to the unloaded control and to the 3 wt% hydrophilic Dox loaded UCA ($p<0.05$) (Figure 6-17). However, the size was still within the criteria since they were less than 5 μm. Figure 6-18 shows that the UCA loaded with 3 wt% h-Dox were more uniform in size than other samples. This uniformity in size was also observed in the SEM images shown in Figure 6-19.

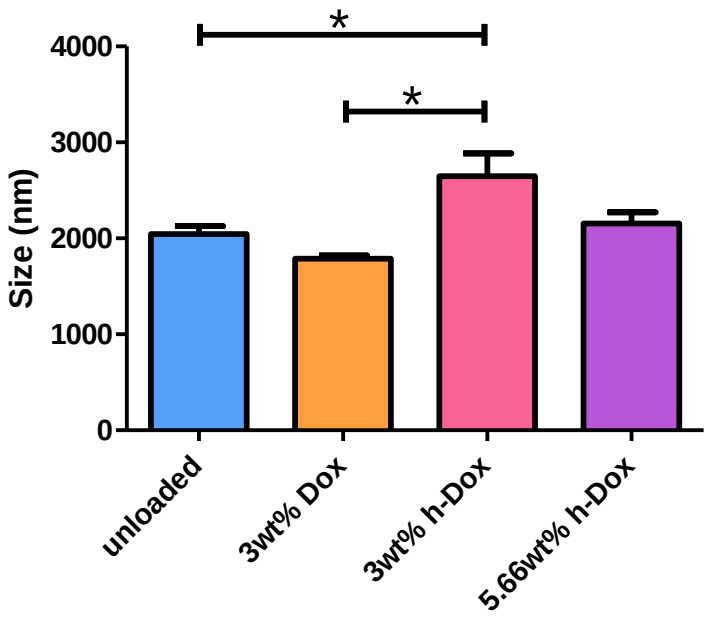

Figure 6-17 The effect of varying the loading of different forms of Dox on the size of UCA (n=3 for all except 5.66wt% h-Dox which has n=1, error bars=SEAM)

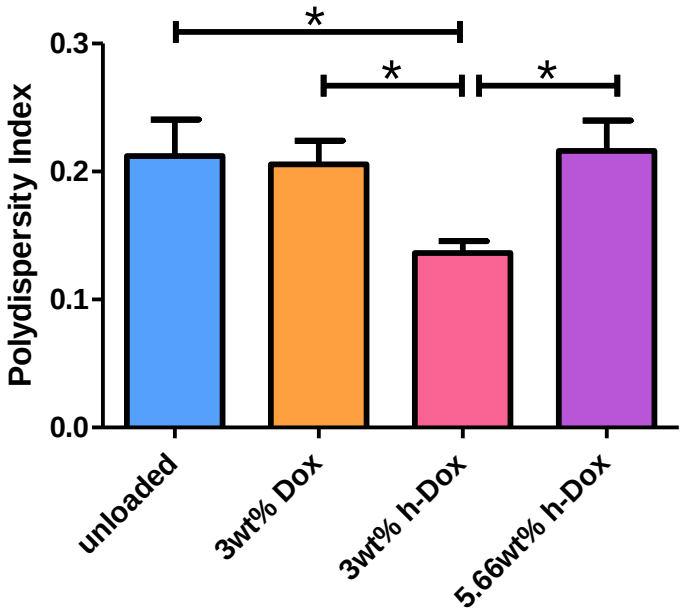

Figure 6-18 The effect of varying the loading of different forms of Dox on the polydispersity index of the UCA (n=3 for all except 5.66wt% h-Dox which has n=1, error bars=SEAM)

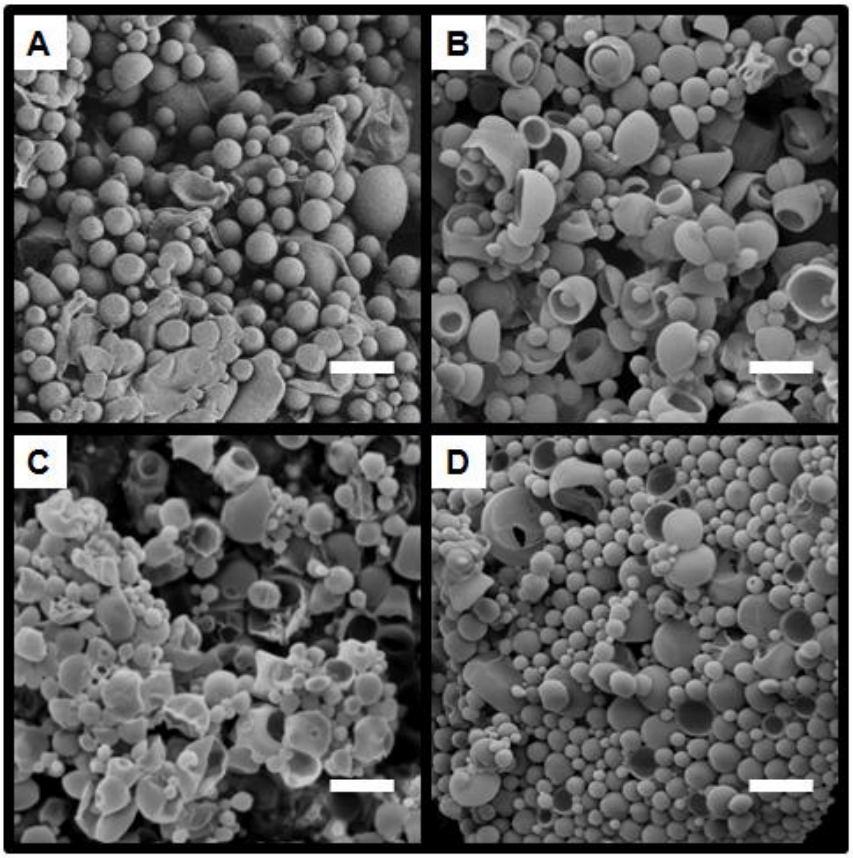

Figure 6-19 SEM images comparing the morphology of the UCA loaded with doxorubicin. Magnification is 3500x. All size bars are 2.5µm. Image (A) blank control UCA (B) 3 wt% hydrophilic Dox (C) 5.66 wt% h-Dox (D) 3 wt% h-Dox

The presence of many poorly formed microbubbles observed in the SEM image of the 5.66 wt% h-Dox loaded UCA could account for the low acoustic enhancement (Figure 6-15). These particles most probably do not have the gas core that could help reflect and scatter the incoming ultrasound waves.

The zeta potentials in Figure 6-20 were unexpected since the hydrophobic and hydrophilic Dox encapsulation was thought to affect the charge of the bubbles formed differently. Both forms had a less negative surface charge than the unloaded UCA. The higher charge on the surface could be due to the Dox which was encapsulated in the shell

was in its hydrophobic form. Hydrophobic compounds would be uncharged so it could have decreased the charge of those h-Dox loaded UCA. The less negativity would make the bubbles more likely to flocculate. However, the zeta potential between the 3 wt% Dox-HCl and 3 wt% h-Dox were not significantly different ($p>0.05$).

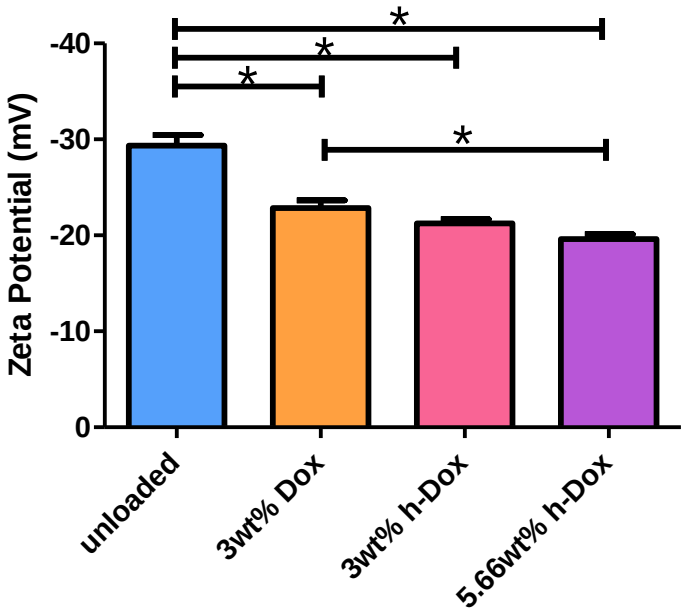

Figure 6-20 The effect of varying the loading of different forms Dox on the zeta potential of UCA (n=3, error bars=SEAM)

7. CONCLUSIONS AND CONTRIBUTIONS TO SCIENCE

In this thesis, increased loading of Dox on PLA UCA was achieved by changing the formulation of the Dox to make it more hydrophobic in order to increase its interaction with the hydrophobic PLA during the encapsulation process. This would increase its therapeutic effectiveness since more Dox could be delivered per μg of UCA injected into the patient and less microbubbles would need to be injected into the body, decreasing their chance of detection by the immune system. This work is in agreement with previous work in this laboratory that showed that hydrophobic drugs such as paclitaxel are encapsulated at higher drug loadings than hydrophilic drugs such as Dox-HCl.

All design criteria and constraints about the acoustic properties, size and surface properties of UCA were met for this h-Dox loaded UCA design. The 3 wt % h-Dox loaded UCA were above the 12 dB cut off for the acoustic enhancement and have an *in vitro* half life of more than 15 minutes. Their size was less than the 5 μm cut-off, allowing them to travel through capillaries without causing embolisms. Their dispersity in size was also low enough to ensure that the size would not reach the 5 μm. In addition, the zeta potential was comparable to the 3 wt% Dox-HCl to ensure that clamping would not occur when administered. These characteristics also make them a functional ultrasound contrast agent and not just a control release agent.

In addition, magnetic nanoparticles can be used to encapsulate Dox but they have a low loading, making them an inefficient way to increase the Dox loading in UCA. In addition, MNP-OA stored in methylene chloride for over a week should not be encapsulated in UCA since they lose their acoustic properties and are no longer dispersed

as expected for capped MNP. Further coating of MNP-OA with Pluronic acid proved to also make the UCA lose their echogenic properties since less spherical microbubbles were formed.

From these experiments where different particles and molecules were loaded onto the wall of the PLA UCA, it was seen that acoustic properties of the UCA can be significantly affected. If MNP were to help increase the loading of Dox on UCA, the design should include the addition of the free h-Dox on the shell as well as the Dox loaded MNP, producing multimodal contrast agents. Other nanocrystals such as gold nanoparticles can also be used as possible agents of increasing Dox encapsulation on UCA.

8. FUTURE RECOMMENDATIONS

Further tests can be carried out to determine the formation of nanoshards and the release of Dox *in vitro* cell cultures. Also, *in vivo* lab animal models can be used to test the actual therapeutic efficiency and possible immune responses to the h-Dox UCA. In order to further increase the Dox encapsulation onto the microbubbles, the maximum mass of hydrophilic Dox that could be loaded into the shell through dissolving the hydrophilic Dox in ammonium carbonate solution should also be explored. The maximum acoustic enhancement and physical properties such as size, zeta potential and PDI should also be determined. This can be used to optimize the amount of Dox-HCl loaded into the ammonium carbonate and the amount of h-Dox loaded inside the shell to get as much drug on the UCA without significantly decreasing their acoustic properties.

The use of MNP in UCA can be used to create a multimodal contrast agent for diagnostic purposes as well as to track the uptake of the nanoshards. In order to make a more echogenic administration of the MNP-OA loaded UCA into the patient, the fabrication method can be optimized to remove unformed small clumps of PLA. A possible method would be cross-flow filtration, or differential centrifugation. Adding more wash steps where the sample can be centrifuged at different revolutions per minute and at different times should also be explored. The effect on the size and size dispersity should be investigated at each stage.

The effect of other capping agents on MNP should also be tested to determine whether this would increase the loading of the Dox compared to this current model of oleic acid and pluronic acid capping. The compound that has hydrophilic ends and a hydrophobic middle can be used as a replacement for pluronic acid and oleic acid and

their acoustic properties can be tested. A combination of Dox loaded MNP and h-Dox encapsulation on the UCA can also be investigated to determine whether more Dox can be loaded.

9. REFERENCES

[1] Fact Sheets by Cancer (2014, August 20). *GLOBOCAN 2012: Estimated Cancer Incidence, Mortality and Prevalence Worldwide in 2012.* Retrieved August 20, 2014, from http://globocan.iarc.fr/Pages/fact_sheets_cancer.aspx

[2] Early Breast Cancer Trialists' Collaborative Group (EBCTCG). (2005). Effects of chemotherapy and hormonal therapy for early breast cancer on recurrence and 15-year survival: an overview of the randomised trials. *Lancet, 365*(9472), 1687–1717. doi:10.1016/S0140-6736(05)66544-0

[3] The Cochrane Collaboration (Ed.). (1996). *Cochrane Database of Systematic Reviews: Reviews*. Chichester, UK: John Wiley & Sons, Ltd. Retrieved from http://www.ncbi.nlm.nih.gov/pubmedhealth/PMH0010915/

[4] Types of Treatment - National Cancer Institute. Retrieved August 22, 2014, from http://www.cancer.gov/cancertopics/treatment/types-of-treatment

[5] *Pechar M, Ulbrich K, Subr V, Seymour LW, Schacht EH.* (2000). *Poly(ethylene glycol) multiblock copolymer as a carrier of anti-cancer drug doxorubicin. Bioconjug Chem.* 11*:*131–*9.*

[6] Crown J, O'Leary M. (2000) The taxanes: an update. *Lancet*. 355:1176–8.

[7] Singer JW, Baker B, De Vries P, et al. (2003). Poly-(*l*)-glutamic acid-paclitaxel (CT-2103) [XYOTAX], a biodegradable polymeric drug conjugate: characterization, preclinical pharmacology, and preliminary clinical data. *Adv Exp Med Biol*. *519*:*81*–99.

[8] J.R. Eisenbrey, O.M. Burstein, R. Kambhampati, F. Forsberg, J.B. Liu, M.A. Wheatley(2010). Development and optimization of a doxorubicin loaded poly(lactic acid) contrast agent for ultrasound directed drug delivery. *J Control Release*.143(1):38-44.

[9] Cancer Facts and Figures 2013 (2013, March 21). *American Cancer Society | Information and Resources for Cancer: Breast, Colon, Lung, Prostate, Skin*. Retrieved June 13, 2013, from http://www.cancer.org/acs/groups/content/@epidemiologysurveilance/documents/document/acspc-036845.pdf

[10] Treatment Types. *American Cancer Society | Information and Resources for Cancer: Breast, Colon, Lung, Prostate, Skin*. Retrieved June 13, 2013, from http://www.cancer.org/treatment/treatmentsandsideeffects/treatmenttypes/index

[11] UPDATE: Chemotherapy side effects. (2012, July 28). *Chemist & Druggist*, 13. Retrieved from http://go.galegroup.com/ps/i.do?id=GALE%7CA298012751&v=2.1&u=drexel_main&it=r&p=AONE&sw=w

[12] Jain, R. K. (1994). Barriers to drug delivery in solid tumors, *Scientific America*, 271, 58-65.

[13] Abraham S. A., Waterhouse D. N., Mayer L. D., Cullis *et al.* (2005).The liposomal formulation of doxorubicin. *Methods in enzymology*, 391, 71-97.

[14] Kaplan, B. W. (2010, August-September). Doxorubicin. *Oncology Nurse Advisor*, 35+. Retrieved from http://go.galegroup.com/ps/i.do?id=GALE%7CA242509614&v=2.1&u=drexel_main&it=r&p=AONE&sw=w

[15] Doroshow, J. H. (1991). Doxorubicin-induced cardiac toxicity. *The New England Journal of Medicine*, *324*(12), 843-845.

[16] Home - United States Biological. Doxorubicin. Retrieved August 20, 2014, from https://www.usbio.net/misc/doxorubicin

[17] Doxil: Drug Description. (n.d.). *RxList*. Retrieved June 13, 2013, from http://www.rxlist.com/doxil-drug.htm

[18] Working P.K., Newman M.S., Sullivan T. *et al.* (1999). Reduction of the cardiotoxicity of doxorubicin in rabbits and dogs by encapsulation in long-circulating, pegylated liposomes. *J Pharmacol Exp Ther.* 289. 1128–1133.

[19] Barenholz, Y. (2012). Doxil® — the first FDA-approved nano-drug: Lessons learned. *Journal of Controlled Release*, 160(2), 117-134.

[20] Chan V., Perlas A. (2011). Basics of Ultrasound Imaging - Springer. Retrieved August 20, 2014, from http://link.springer.com/chapter/10.1007%2F978-1-4419-1681-5

[21] Leighton T. G.(2007). What is ultrasound? *Progress in Biophysics and Molecular Biology*, 93, 3-83.

[22] Hoff L. (2001). Acoustic Characterization of Contrast Agents for Medical Ultrasound Imaging, Kluwer Academic Publishers, Netherlands. 1-2.

[23] Hogg J. (1987) Neutrophil kinetics and lung injury. *Phisiology Review* 67, 1249-1295.

[24] Hasik M. J., Kim D. H., Howle L. E., Needham D., and Prush D. P.(2002), Evaluation of synthetic phospholipid ultrasound contrast agents, *Ultrasonics*, 40, 973-982.

[25] Zhao Y. Z., Luo Y. K., Zhang Y., Mei X. G., and Tang J., (2005) Property and contrast-enhancement effects of lipid ultrasound contrast agent: A preliminary experimental study, *Ultrasound in Medicine & Biology*, 31, 537-543.

[26] Díaz-lópez R., Tsapis N., and Fattal E., (2010) Liquid Perfluorocarbons as Contrast Agents for Ultrasonography and 19F-MRI, *Pharmaceutical Research*, 27, 1-16.

[27] Bertolotto M, Catalano O. (2009). Contrast-enhanced ultrasound: past, present, and future. *Ultrasound Clinics*. 4(3), 339-67.

[28] Ultrasound Contrast Agents. Retrieved September 3, 2014, from http://www.icus-society.org/about-ceus/ultrasound-contrast-agents

[29] Ultrasound Contrast Agents -- commercially available outside the United States. Retrieved September 3, 2014, from http://www.icus-society.org/about-ceus/ultrasound-contrast-agents/231-ultrasound-contrast-agents-commercially-available-outside-the-united-states

[30] Sonazoid (TN) - PubChem. Retrieved September 3, 2014, from http://pubchem.ncbi.nlm.nih.gov/summary/summary.cgi?sid=47207110

[31] Maresca, D., Emmer, M., van Neer, P. L. M. J., Vos, H. J., Versluis, M., Muller, M., van der Steen, A. F. W. (2010). Acoustic sizing of an ultrasound contrast agent. *Ultrasound in Medicine & Biology*, *36*(10), 1713–1721. doi:10.1016/j.ultrasmedbio.2010.06.014

[32] DEFINITY® Frequently Asked Questions. Retrieved September 3, 2014, from http://www.definityimaging.com/how-faq.html

[33] Natural Fibre Bio-Composites Incorporating Poly(Lactic Acid) | InTechOpen. (n.d.). Retrieved August 20, 2014, from http://www.intechopen.com/books/fiber-reinforced-polymers-the-technology-applied-for-concrete-repair/natural-fibre-bio-composites-incorporating-poly-lactic-acid-

[34] Lensen D., Gelderblom E.C., Vriezema D.M. *et al.* (2011). Biodegradable polymeric microcapsules for selective ultrasound-triggered drug release. Soft matter, 7 , 5417-5422.

[35] Eisenbrey, John. (2010). Ultrasound Sensitive Polymeric Drug Carriers for Treatment of Solid Tumors. *PhD Thesis, Drexel University Department of Biomedical Engineering, Science & Health Systems, Philadelphia*.

[36] Yezhelyev M.V., Gao X., Xing Y. *et al.* (2006). Emerging use of nanoparticles in diagnosis and treatment of breast cancer.*Lancet Oncol*, 7, 657–667.

[37] Choi H. S., Liu W, Misra P. *et al.* (2007). Renal Clearance of Nanoparticles. *Nat Biotechnol*. 25(10), 1165-1170.

[38] Hobbs S. K., Monsky W.L., Yuan F. *et al.* (1998). Regulation of transport pathways in tumor vessels: Role of tumor type and microenvironment. *Proceedings of the National Academy of Sciences*, (95), 4607–4612.

[39] Haley, B., & Frenkel, E. (2008). Nanoparticles for drug delivery in cancer treatment. *Urologic Oncology: Seminars and Original Investigations*, 26(1), 57-64.

[40] Marinescu M. Langer M. *et al.* (2013). Synchrotron Radiation X-Ray Phase Microcomputed Tomography as a New Method to Detect Iron Oxide Nanoparticles in the Brain. *Mol Imaging Biol.*

[41] Lam T., Pouliot P., *et al.* (2013). Superparamagnetic Iron Oxide Based Nanoprobes for Imaging and Theranostics. *Advances in colloid and Interface Science.* Accepted Manuscript.

[42] Bjornerud A., Johansson L. (2004). The utility of superparamagnetic contrast agents in MRI: theoretical consideration and applications in the cardiovascular system. *NMR Biomed.* 17(7), 465-477.

[43] Sun. C., Lee J. S., *et al.* (2008). Magnetic nanoparticles in MR imaging and drug delivery. *Adv. Drug Delivery.* 60(11), 1252-1265.

[44] Niu C., Wang Z., Lu G., *et al.* (2013). Doxorubicin loaded superparamagnetic PLGA-iron oxide multifunctional microbubbles for dual-mode US/MR imaging and therapy of metastasis in lymph nodes. *Biomaterials.* 34, 2307-2317.

[45] Kievit F. M., Wang F. Y., *et al.* (2011). Doxorubicin loaded iron oxide nanoparticles over multidrug resistance in cancer in vitro. *J Control Release.* 152(1), 76-83.

[46] Oleic acid ≥99% (GC) | Sigma-Aldrich. Retrieved August 20, 2014, from http://www.sigmaaldrich.com/catalog/product/sial/o1008?lang=en&region=US

[47] fig4a.gif (GIF Image, 902 × 174 pixels). Retrieved August 20, 2014, from http://www.nmr.unsw.edu.au/guide/nmr/druganal/images2/fig4a.gif

[48] Liu, X., Kaminski, M. D., Chen, H., Torno, M., Taylor, L., & Rosengart, A. J. (2007). Synthesis and characterization of highly-magnetic biodegradable poly(d,l-lactide-co-glycolide) nanospheres. *Journal of Controlled Release*, *119*(1), 52–58. doi:10.1016/j.jconrel.2006.11.031

[49] Jain, T. K., Morales, M. A., Sahoo, S. K., Leslie-Pelecky, D. L., & Labhasetwar, V. (2005). Iron oxide nanoparticles for sustained delivery of anticancer agents. *Molecular Pharmaceutics*, *2*(3), 194–205. doi:10.1021/mp0500014

[50] Kataoka, K., Matsumoto, T., Yokoyama, M., Okano, T., Sakurai, Y., Fukushima, S., Kwon, G. S. (2000). Doxorubicin-loaded poly(ethylene glycol)-poly(beta-benzyl-L-aspartate) copolymer micelles: their pharmaceutical characteristics and biological significance. *Journal of Controlled Release: Official Journal of the Controlled Release Society*, *64*(1-3), 143–153.

[51] Sherif D. E., Wheatley M. A. (2003) Development of a novel method for synthesis of a polymeric ultrasound contrast agent. *J. Biomedical Mat. Res.* 66(A), 347-355.

[52] Oum, Kelleny. (2008). Therapeutic and diagnostic applications of ultrasound contrast media for breast, ovarian and skin cancers. *PhD Thesis, Drexel University Department of Biomedical Engineering, Science & Health Systems, Philadelphia*.

[53] Cochran, M. C., Eisenbrey, J., Ouma, R. O., Soulen, M., & Wheatley, M. A. (2011). Doxorubicin and paclitaxel loaded microbubbles for ultrasound triggered drug delivery. *International Journal of Pharmaceutics*, *414*(1-2), 161–170. doi:10.1016/j.ijpharm.2011.05.030

[54] Yeh C.K., Yang M.J., and Li P.C., (2003).Contrast-specific ultrasonic flow measurements based on both input and output time intensities, *Ultrasound in Medicine & Biology*, 29. 671-678.

[55] Forsberg F., Lathia J.D., Merton D.A., Liu J., Le N., Shimizu M., Goldberg B.B. and Wheatley M.A. (2004). Effect of Shell Type on the In Vivo Backscatter from Polymer Encapsulated Microbubbles. *Ultrasound Med Biol.*, 30(10). 1281-1287.

[56] Khemani M., Sharon M., and Sharon M. (2012). pH Dependent Encapsulation of Doxorubicin in PLGA, *Annals of Biological Research*, *3* (9), 4414-4419.

10. APPENDIX

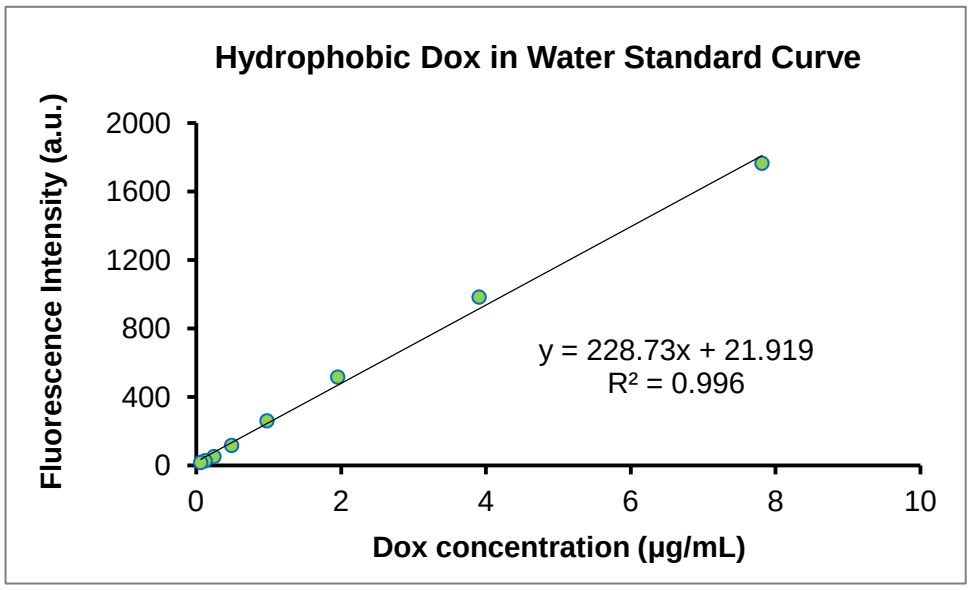

Figure 10-1 Standard curve of h-Dox in water used to calculate the encapsulation efficiency on MNP capped with oleic acid and coated with pluronic acid (n=3, error bars=SEAM)

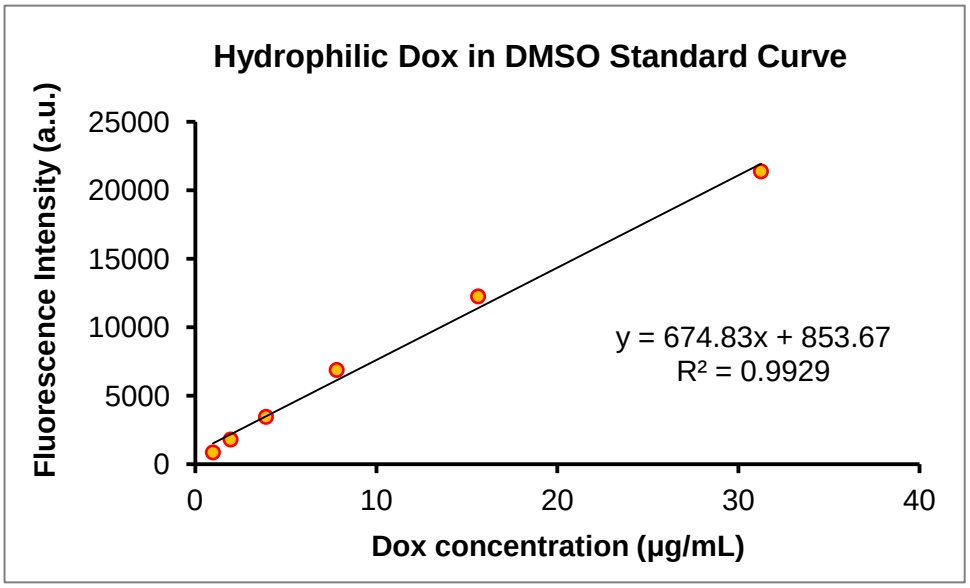

Figure 10-2 Standard curve of hydrophilic Dox in DMSO used to calculate the encapsulation efficiency on UCA (n=3, error bars=SEAM, Ex= 495nm, Em= 585nm, Gain=118 dB)

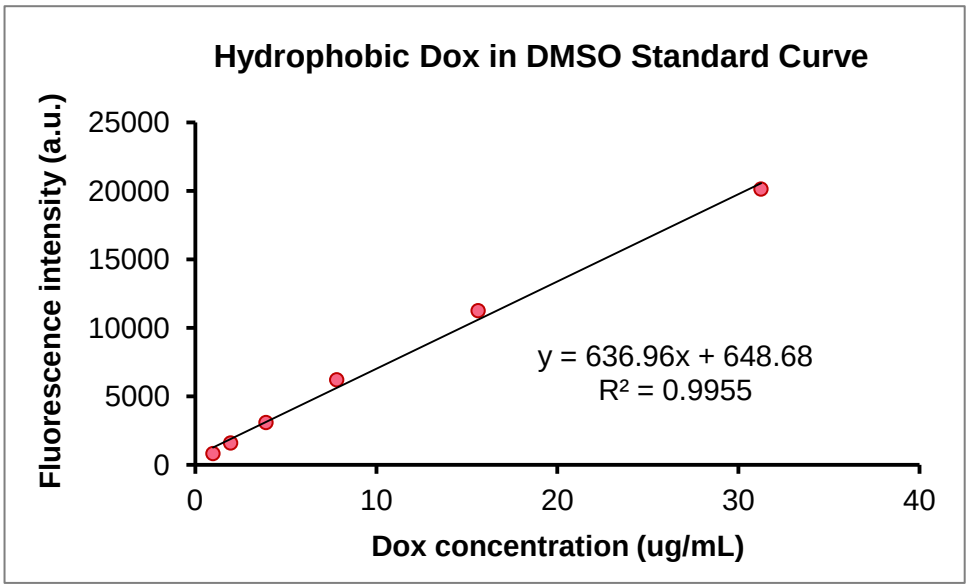

Figure 10-3 Standard curve of h-Dox in DMSO used to calculate the encapsulation efficiency on UCA (n=3, error bars=SEAM, Ex= 485nm, Em= 591nm, Gain=120 dB)